POLYTECHNIC UNIVERSITY OF MARCHE

SCHOOL OF MEDICINE

Doctorate Program in "Human's health"

Cyclical, dynamic chromatin and redox changes trigger and sustain Epithelial Mesenchymal Transition induced by TGF-β1

Tutor:

Prof. Armando Gabrielli

PhD candidate:

Jacopo Dolcini

XXIX cycle 2013/2016

INDEX

A Rosaria

1.INTRODUCTION

1.1THE EPITHELIAL-MESENCHYMAL TRANSITION

The epithelial-mesenchymal transition (EMT) is a complex biological program in which epithelial cells gradually lose their epithelial characteristics and acquire a phenotype with mesenchymal features. These characteristics can be summarized as loss of cell polarity and cell-cell adhesion; acquisition of migratory and invasive capacity and expression of proteins such as Vimentin, fibronectin and N-cadherin. The first demonstration of the ability of epithelial cells to acquire mesenchymal characteristics such as the absence of cell polarity and migration capabilities, was described in 1982 by Greenburg and Hay[1]. Since then, the knowledge and the number of information concerning EMT have increased exponentially. There is evidence that EMT plays a key role in both physiological and pathological processes[2]. From a functional biological point of view, EMT is divided into three main types: Type I, during embryogenesis; Type II, during tissue repair; Type III, in the metastatic spread of cancer[3]. All three types are however united by the acquisition by epithelial cells of migratory ability and loss of adhesion and cell polarity.

The first critical step is represented by the loss of various cellular markers; there is a significant reduction in E-cadherin, a protein responsible for cell-cell side interactions by tight junctions and adhesion and relative immobility of the epithelial cells to the tissue structure[4]. The down-regulation of this protein is also mediated by increased expression of vimentin which reduces the transport of the E-cadherin at the cell surface. Parallel to this, during EMT, the cell acquires the ability to express a protein pattern characterized by N-cadherin, fibronectin and matrix metalloproteinases that typically characterize the

mesenchymal phenotype[5]. The expression of fibronectin and the loss of a polarized cytoskeleton allow epithelial cell the acquisition of motility[6]. It's important to note that EMT, in many instances, is a mix of epithelial and mesenchymal phenotypes: cells lie along a gradient of incomplete transition where both epithelial and mesenchymal features coexist[7].

1.2 EMT AND PHYSIOLOGY

EMT has been described as a fundamental process in important physiologic events such as wound healing and organ repair[8]. Many models of cutaneous wound healing have shown that wound healing is a multi-step process which involves inflammatory response associated with cell proliferation, migration and ECM remodeling. In fact, during wound healing, keratinocytes at the wound edge lose their intercellular adhesion and migrate across the wound. Specifically, these keratinocytes undergo changes in junctional complexes including a reduction in desmosomes and adherent junctions, a disruption of intermediate filaments and cytoskeletal reorganization that results in the creation of intercellular gaps. These modifications change the morphology of keratinocytes and let them acquire motility and shape features mesenchymal like[9,10]. In addition has been shown that Slug, one of the main EMT transcription factor, is involved in re-epithelialization and keratinocytes migration and motility; healing of excisional wounds is impaired in Slug knockout mice[11] and keratinocytes from these mice show a defect of migration and motility at the wound hedge[12]. In fact, Slug regulates keratinocytes during re-epithelialization by repressing E-cadherin then leading to reduced cell-cell adhesion and desmosome disruption.[13,14]

EMT has also been described as a fundamental process in extra cutaneous organs development and repair: in hearth, EMT progress of epicardial and myocardial cell line is very important for a normal development as demonstrated by generation of knockout mice for TGFβ type2 receptor, one of the main signaling pathway of EMT, that led to hearth defects and vascular abnormalities such as ventricular myocardium hypoplasia, septal defects and irregularities of descending thoracic aorta[15].

EMT program is also activated in hearth after myocardial ischemic or mechanical injury as demonstrated in mouse and zebrafish[16].

1.3EMT AND PATHOLOGY

1.3.1 EMT AND FIBROSIS

Many evidences have shown the role of EMT in complex pathological processes as fibrosis and metastatic spread of cancer.

During wound-healing physiologic repair, tissue integrity could be restored not only by re-epithelization but also through formation of a stress-resistant scar. This process is orchestrated by myofibroblast and a pathologically prolonged activity of them results in fibrogenesis. Indeed, persistent myfibroblast activation is a shared feature of fibrotic disease[17]. Dysregulation of EMT process is one of the elements that can to support and to contribute to fibrosis in multiple organs.

In kidney, a chronic disease may cause interstitial fibrosis that could lead to loss of function until end-stage renal failure. Many studies have shown the involvement of EMT program in renal fibrosis, showing that fibroblasts responsible for fibrogenesis in a murine model could derive both from bone marrow and both from local EMT[18]. In vivo have also been reported presence of EMT markers in human renal biopsies[19].

Many evidences show that one of the main inducer of EMT in renal fibrosis is TGFβ1, an isoform of TGβ family, which is involved in renal tubular epithelial EMT[20].

Moreover, in lung, persistent and repeated injury may lead to persistent inflammation and activation of EMT and then fibrosis[21]. Many studies and murine models have investigated the occurrence of EMT in lung fibrosis, partially mediated by TGFβ1[22,23].

Hearth is another organ where EMT plays a role following cardiac injury: adult epicardium derived cells have shown the possibility to undergo EMT and migrate into injured myocardium, where they may produce various cell types as interstitial fibroblast and coronary smooth muscle cells[24,25] involved in cardiac repair process.

Also hepatic fibrosis may be mediated by EMT; in fact has been shown that TGFβ may induce EMT in hepatocytes in vitro through the activation of TGFβ1/Smad pathway[26].

1.3.2 EMT AND CANCER

Close connection between EMT and cancer progression is known since more than ten years[27]. Many EMT transcription factors are involved not only in acquisition of migration and invasive capacities, but also in suppression of cell senescence and apoptosis and resistance to radiotherapy and chemotherapy[28,29]. Cells undergoing EMT may contribute to immunosuppression and act as cancer stem-like cells[30]. Therefore, with EMT, cancer cells may acquire a general more aggressive phenotype, the possibility to metastasize and the activation of EMT in tumor primaries cells can be induced by stimuli from tumor microenvironment[31]. Indeed EMT may be promoted by hypoxia, low ph, mechanical stress, adaptive and innate immune response, altered extracellular matrix and treatment with antitumor drugs. One important element is that EMT can induce many epigenetic changes as, in example, methylation of E-cadherin gene promoter region[32]. These changes are inheritable and may persist also if the original stimulus is no longer present.

EMT can be induced also by stimulus independent elements, as constitutive receptor activation, activating mutations of intracellular pathways elements as Janus kinase 2 (JAK2), phosphoinositide 3-kinase catalytic subunit-α (PIK3CA), BRAF or KRAS, together with inactivating mutations or deletions of tumor suppressors such as Von Hippel-Lindau disease tumor suppressor (VHL) or phosphatase and tensin homologue (PTEN)[33].

This combination of stimulus dependent and independent activation can increase EMT potential.

It is important to underline that EMT it's not an-all-or-nothing event whereby tumor cells lose entirely their epithelial markers to acquire exclusively mesenchymal features; the process is the result of a complex crosstalk between

tumor cells, tumor associated cells and stroma, a crosstalk mediated by paracrine and autocrine factors[34]. In many solid tumors, tumor associated cells play a pivotal role in progression of EMT: recently has been show how cancer associated fibroblast (CAF), can promote metastatic propensity of colon rectal cancer by secreting cytokines and increasing cancer-stem like cells (CSC) by inducing features of EMT and reprogramming of cancer progenitors into CSCs[35]

1.4 EMT SIGNAL TRANSDUCTION PATHWAYS

There are many growth factors involved in starting and progression of EMT; these growth factors such as epidermal growth factor (EGF), fibroblast growth factor (FGF), hepatocyte growth factor (HGF) and transforming growth factor β (TGFβ1) are both involved in physiological processes involving EMT such as wound healing and organ repair and pathological processes. FGF, EGF and HGF function as ligands for their corresponding receptors, which are tyrosine kinase trans-membrane receptors resulting in their dimerization and autophosphorylation[36]. This can lead to activation of pathways such as MAPK, p38 MAPK, JNK and others causing upregulation of EMT transcription factors like Snail, Slug and ZEB[37].

TGFβ pathway is probably the most studied EMT pathway; TGFβ is a superfamily that comprises many proteins such all TGFβ isoforms, bone morphogenetic proteins (BMPs), activins and others. TGFβ isoforms are three: TGFβ1, TGFβ2 and TGFβ3. Their role has been widely investigated in cell proliferation, migration and differentiation[38]. The functional complex of TGFβ receptors at cell surface consists of two type II and two type I transmembrane

serine/threonine kinase receptors. Only five type II receptors and seven type I receptors have been identified for 29 different ligands[39]. In the absence of ligand type II and type I receptors exist as homodimers at cell surface. Each ligand can bind to different combinations of type II and type I receptors: i.e. TGFβ1, TGFβ3 and activins bind their type II receptors without needing a type I receptor, whereas BMP2, BMP4 and BMP7 bind primarily to their type I receptors, BMP-RIA or BMP-RIB, although heteromeric BMP receptors complexes provide higher-affinity ligand binding[40]. Otherwise, TGFβ2 interacts only with type I and type II receptor combinations.

It is worth to stress that although this pathway is inherently simple there is a more complex versatility in receptor interactions and ligand binding; these interactions may modulate TGFβ signaling and orchestrate his Smad dependent or independent response[41].

Smad family, small mother against decapentaplegic, is one of the main effector of TGFβ signaling; there are eight vertebrate Smad, Smad1 to Smad8. Smad2 and Smad3 are activated through carboxyl-terminal phosphorylation by TGFβ and interaction with TβRI and ActRIB receptors, whereas Smad1, Smad5 and Smad8 are activated by ALK-1, ALK-2, BMP-RIA/ALK-3 and BMP-RIB/ALK-6 in response to BMP or other ligands[42,43]. These receptor-activated Smads (R-Smads) are released from the receptor complex to form a heterotrimeric complex of two R-Smads and a common Smad4, and translocate into the nucleus[44]; instead, Smad6 and Smad7 act as inhibitory Smads[45]. The increment of Smad6 and Smad7 caused by TGFβ and BMP represents an auto-inhibitory feedback mechanism for ligand induced signaling[46].

After activation, Smad complexes may go into the nucleus where they regulate gene expression. Nuclear import of R-Smads does not require Smad4, although Smad4 co-translocates with R-Smads. Final effect of this import is physical

interaction and functional cooperation of DNA binding Smads with sequence specific transcription factors and co-activators[47].

Many genes are activated in response to TGFβ ligands while others are repressed; specifically TGFβ represses c-Myc and Id family members. Of course, this repression is mediate with the cooperation of other transcription factors as E2F4, E2F5 and p107: this complex is pre-assembled in cytoplasm and then, after stimulation with TGFβ, translocates into the nucleus where, in association with Smad4, it binds to a Smad-E2F-binding site in c-Myc promoter and represses c-Myc expression[48].

TGFβ inhibits also myoblast, osteoblast and adipocyte differentiation and it is very interesting how Smads can repress or activate transcription depending on cell types: as an example, Smad3 cooperates with Runx proteins to activate transcription in epithelial cells and repress transcription from the same promoter in mesenchymal cells[49].

Besides Smad-mediated transcription, TGFβ mediates other signaling cascades including MAPK pathways, Erk, JNK but how they are activated and their biological effects are still poor characterized[50]. It's possible to hypothesize that these different pathways can amplify themselves and regulate each other: TGFβ induced activation of Erk and JNK can result in Smad phosphorylation and regulate Smad activation[51,52].

The dual ability of TGFβ to activate Smads and MAPK signaling has a role in EMT and although this convergence often results in cooperativity, these pathways may counteract each other[53,54].

1.5 EMT: TRASCRIPTION AND EPIGENETIC FEATURES

Epigenetics has been traditionally described as the amount of mechanisms that can determine cellular phenotypes without concomitant changes in the genome of a cell, specifically without changes in its nucleotide sequences. Recently the term has gain a new and wider meaning, since epigenetic modifications can be achieved by many mechanisms and, among these, may be included methylation of cytosine residues and covalent modifications of the histone proteins that form DNA associated nucleosomes.[55] In the last ten years, modifications which can generate active or repressive histone marks that are catalyzed by a variety of histone modifying enzymes, has been recognized as fundamental process of gene regulation[56]. For example, histone methyltransferases and demethylases can either add or remove methylation marks on the lysine residues of nucleosome subunits, especially those of histones H3 and H4. These chemical reactions play an important role how DNA is packaged in chromatin, determining the transcriptional potential of underlying genes. Recently, many studies have shown the connection between EMT transcription factors (EMT-TFs) activation and histone modifications. For example, many EMT-TFs are recruited to the promoter of CDH1, the gene codifying for E-cadherin, and repress its transcription after activation of EMT program[57].

In recent years, many studies have begun to link the lysine-specific demethylase, LSD1, to EMT; LSD1 was the first histone demethylase to be identified and was initially shown to remove methyl groups from the transcription-activating H3K4me3 mark[58]. It's should be noted that in breast cancers LSD1 is highly expressed in estrogen receptor and negative tumor, which tend to bring mesenchymal gene features and this can support its role in promoting EMT[59].

LSD1 overexpression has been correlated both with poor survival in many types of cancer and both with inhibition of invasiveness and metastatic potential[60,61]; these apparently controversial role may be attributed to the fact that LSD1 is able to modify multiple histone lysine substrates. Apart from converting active H3K4me2 or H3K4me3 to the less active H3K4me1 mark, LSD1 is now known to cause demethylation of the inactive H3K9me3 mark, converting it into the less repressive H3K9me1 or H3K9me2 marks, thereby causing gene de-repression[62].

So, the functional activity of LSD1 is determined by a balance between gene activation and repression based on its capacity to modify H3K4me3, H3K9me3 or both.

Referring to this bivalence, certain segments of DNA may be associated with facultative heterochromatin, implying an ability to alternate between induced and repressed states of expression. Facultative heterochromatin, associated with H3K27me3, can be easily converted in an active euchromatinic state[63]. So this bivalent configuration of certain EMT associated genes may explain the rapid and reversible change between epithelial and mesenchymal state that some epithelial cells could have during EMT process[64,65].

This wide involvement of various histone-modifying enzymes reflects the characteristic of EMT program as a succession of changes as cell pass from a fully epithelial phenotype to a fully mesenchymal one, sustained by a spectrum of progressively more stable epigenetic changes[66].

1.6 SNAIL AND WIF1

SNAI1, also known as SNAIL, is a zinc finger protein encoded in humans by SNAIL gene[67]. Initially this transcription factor, the first member of superfamily SNAIL, has been described in Drosophila Melanogaster[68] and has been studied in relation to his role in morphogenesis, as it is essential for mesoderm formation in several organism from flies to mammals[69]. Recently his role has been evaluated also in processes that require large-scale cell movements such as the formation of neural crest and EMT.

To confirm his central role in EMT two different approaches has been used: first Snail was shown to convert normal epithelial cells into mesenchymal cells through the direct repression of E-cadherin[70,71]. Moreover is direct effect on E-cadherin repression is very important in normal progression of embryos development which requires EMT program. SNAIL knockout animals die at gastrulation stages and show defects in EMT[72]. Of course, E-cadherin is the principal target of SNAIL but not the only one: it can downregulate others epithelial marker such as desmoplakin, the epithelial mucin Muc-1 and cytokeratin-18 and is able to upregulate and to redistribute mesenchymal markers such as vimentin and fibronectin[73].

His involvement in EMT has been demonstrated both in physiological and pathological processes: his overexpression has been found in cell types that were highly invasive and metastatic. Cell lines derived from breast cancer, colon cancer, bladder cancer and melanomas has been analyzed: high levels of SNAIL mRNA were detected in breast cell line and melanoma cell line, while there were low or undetectable expression of E-cadherin in breast, colon and bladder cells[74].

WIF1, Wnt inhibitory factor 1, is a 379 amino acids highly conserved protein. Structurally it consists of an N-terminal signal sequence, a single domain WIF (WD) that mediates the interaction with Wnt and five EGF-like domains. The evolutionary process has selected and preserved this protein along the various evolutionary chains and indeed, it can be found in fish, amphibians, and mammals. In humans it was identified for the first time in retina[75] and the highly conserved homologues were found in the mouse; particularly the expression of WIF1 in the mouse appears to be at the highest levels in heart, lung and at lowest levels in brain and eye[76].

Together with secreted related frizzled proteins, sFRP, WIF1 is a secreted inhibitor of Wnt pathway.

Wnt proteins are a family of proteins that control the activation of several pathways[77]. The principal and more studied pathway activated is Wnt/β-catenin: this pathway, that causes a stabilization of β-catenin and his consequential translocation into cellular nucleus, activate many β-catenin related genes.

The over expression of this pathway is involved in important pathological processes as cancer[78], aging[79] and fibrosis[80].

As a confirmation of this, WIF1 has been founded suppressed in many different pathologies: its promoter region it is methylated in many tumors as nasopharyngeal and esophageal carcinomas[81], lung cancer[82], bladder cancer, breast and prostate cancer[83]. Recently, WIF1 silencing has been found in fibrosis and systemic sclerosis but in this pathology, the gene is silenced through histone deacetylation[84].

Studying Wnt/β-catenin pathway and its inhibitors is very important since its correlation with EMT and with pathologies as cancer and fibrosis where EMT plays an important role[85]

2. AIM OF THE PROJECT

Over last 5-10 years, there has been an increase in the number of reports on the role of reactive oxygen species, ROS, in mediating EMT and supporting tumor growth by activating multiple pathways[86,87]. It's also well established that high ROS levels, characterizing tumors microenvironment, can promote differentiation of myofibroblast into cancer associated fibroblast, also known as CAF[88,89]. These CAFs, through production of cytokines and proteinases, support the activation and progression of EMT[90].

ROS have also been found involved in DNA oxidation, which it has been demonstrated to be essential for the assembly of a productive transcriptional initiation complex. In fact, it's has been shown that under estrogen stimulation LSD1, a FAD oxidase, causes demethylation of histone 3 and its activity produces bursts of nuclear ROS, causing DNA oxidation[91,92] and starting transcription.

In this scenario, the aim of this work is to explore if a similar mechanism, involving ROS, could be the driving force of the transcriptional program leading to EMT in mammary epithelial cells.

To this end, attention has been focused on transcription of two prototypic TGFβ1 activated or repressed gene: SNAIL1, encoding a transcription factor TGFβ1 induced, essential for EMT, and WIF1, encoding a secreted WNT inhibitory factor, downregulated by TGFβ1. WIF1 by inhibiting WNT represses EMT. Recently, it has been found that WIF1 is silenced by ATM checkpoint kinase, activated by oxidative DNA damage[93].

3. MATERIALS AND METHODS

Materials. PVDF membrane was from Millipore (Bedford, MA, USA); anti-ECadherin, anti-Actin, anti-N-Cadherin, anti-LSD1, anti-JMJD2A, anti JMJD2A and anti-SMAD2/3 antibodies were from Santa Cruz Biotechnology (Santa Cruz Biotech,CA, USA); anti-smooth muscle actin antibody and Phalloidin-TRITC were from Sigma-Aldrich (St. Louis, MO, USA); DCFDA and Alexa 488 secondary antibody were from Molecular Probes; anti-H3K4me2, anti-H3K9me3 and anti-Pol 2 antibodies were from AbCam (Cambridge, UK); Oxy-DNA assay was from Calbiochem (S.Diego, CA, USA) ; LSD1 and JMJD2A SiRNA were from Qiagen (Valencia, CA,USA).

Cell Cultures and Transfections. MCF-10A cells were from the American Type Culture Collection (ATCC). MCF10A cells were cultured in DMEM/HAM'S F12 supplemented with 5% horse serum, 0.5 ug/ml hydrocortisone, 100 ng/ml cholera toxin, 20 ng/ml EGF, 10 ug/ml insulin. MCF-10A cells were transfected with plasmids encoding LSD1 or LSD1 mutants using Lipofectamine 2000 (Invitrogen, Waltham, MA, USA) according to manufacturer's instruction or by electroporation**.**

Immunoprecipitation and Immuno-Blot Analysis. 1 × 106 cells were lysed for 20 min on ice in 500 µl of complete RIPA lysis buffer (50 mM Tris-HCl, pH 7.5, 150 mM NaCl, 1% Nonidet P-40, 2 mM EGTA, 1 mM sodium orthovanadate, 1 mM phenylmethanesulfonyl fluoride, 10 µg/ml aprotinin, 10 µg/ml leupeptin). Lysates were clarified by centrifugation and immunoprecipitated for 4 h at 4°C with 1–2 µg of the specific antibodies. Immune complexes were collected on protein A-Sepharose, separated by SDS-PAGE, and transferred onto nitrocellulose. Immunoblots were incubated in 3% bovine serum albumin, 10 mM Tris-HCl, pH 7.5, 1 mM EDTA, and 0.1% Tween 20 for 1 h at room temperature, probed first with specific antibodies and then with secondary antibodies. Quantity-One software was used to perform quantitative analyses.

Real-Time PCR. Total RNA from MCF-10A was extracted using RNeasy (Qiagen, Valencia, CA, USA) according to the manufacturer's instruction. cDNA was synthesized using a high capacity cDNA reverse transcription kit (Applied Biosystem, Foster City, CA, USA) using 1 μg of total RNA. For quantification of mRNA expression, Real-Time PCR reactions were performed on a 7500 Fast Real Time PCR system (Applied Biosystem, Foster City, CA, USA). The primers were:

SNAIL1 (forward): 5'-GAGGCGGTGGCAGACTAG -3';

SNAIL1 (reverse): 5'-GACACATCGGTCAGACCAG -3';

LSD1 (forward): 5'-GAGGCGGTGGCAGACTAG -3';

LSD1 (reverse): 5'-GACACATCGGTCAGACCAG-3';

JMJD2A (forward): 5'-CCAGAACCAACCAGGAGC-3';

JMJD2A (reverse): 5'-TTCACTGCGCGAGACCAT-3'.

Data are normalized to those obtained with β 2-microglobulin primers. Results (mean ± SD) are the mean of three different experiments.

Immuno-cytochemistry. After washing with PBS, cells were fixed with 3.7% formaldehyde solution in PBS for 20 min at 4 °C. After extensive washing in PBS, cells were permeabilized with 0.1% Triton X-100 in PBS and then stained with anti E-cadherin antibody overnight and with 50 μg/ml fluorescent phalloidin conjugate, phalloidin-TRITC, in PBS for 1 h at room temperature and then with anti rabbit Alexa 488 secondary antibodies. After washing with PBS, the cover slides were mounted with glycerol plastine and then observed under a confocal fluorescence microscope (Leica).

8-oxo-G test. After stimulation, cells were fixed with 3% formaldehyde solution in PBS and permeabilized with 0.1% Triton X-100 in PBS. Cells were then incubated with FITC-conjugate probe that binds to 8-oxoguanine for 1h at 37°C. After extensive washing cells were mounted with glycerol plastine and observed at confocal miscroscope.

Intracellular ROS determination. Production of intracellular H2O2 was assayed as previously described (13). At 3 min before the end of the incubation time, DCF-DA was added to a final concentration of 5μM. Cells were lysed in **1ml** of RIPA buffer and analyzed immediately by fluorescence analysis using a Perkin Elmer Fluorescence Spectrophotometer 650-10S equipped with a Xenon Power Supply (excitation 488 nm, emission 510 nm).

Chromatin Immunoprecipitation. MCF-10A cells were grown to 95% confluence in DMEM/Ham's F12. Following the addition of 10 ng/ml TGF-β1 for 2 hours (to evaluate the state of H3K9me3 on SNAIL1 promoter) or for 30 min (to evaluate the state of H3K4me2 on SNAIL1 promoter), cells were washed twice with PBS and cross-linked with 1% formaldehyde at room temperature for 10 min. Cells then werewashed with ice-cold PBS containing protease inhibitors (1 mM phenyl-methylsulphonyl-fluoride (PMSF), 1 μg/ml aprotinin and 1 μg/ml pepstatin-A. Cells were then resuspended in 0.2 ml of lysis buffer (1% SDS, 10 mM EDTA, 50 mM Tris-HCl, pH 8.1, 1mM PMSF, 1 μg/ml aprotinin and 1 μg/ml pepstatin-A, sonicated for 170 cycles (12 sec followed by 28 sec of stop) and centrifuged for 10 min at 10000 x g at 4°C. Supernatants were collected and diluted in buffer containing 1% Triton X-100, 2 mM EDTA, 150 mM NaCl, 20 mM Tris-HCl, pH 8.1. Immunoprecipitation was performed overnight at 4°C with 2 µg of specific antibodies with 14 µl Protein G-Dynabeads (Invitrogen, Waltham, MA, USA). After immunoprecipitation, precipitates were washed sequentially for 10 min each in High Salt Solution (0.1% SDS, 1% Triton X-100, 2 mM EDTA, 20 mM Tris-HCl, pH 8.1, 150 mM NaCl), Low Salt Solution (0.1%SDS, 1% Triton X-100, 2 mM EDTA, 20 mM Tris-HCl, pH 8.1, 500 mM NaCl), and LiCl Solution (0.25 M LiCl, 1% NP-40, 1% deoxycholate, 1 mM EDTA, 10 mM Tris-HCl, pH 8.1). Precipitates were then washed three times with TE buffer and extracted two times with 1% SDS, 0.1 M NaHCO3. Eluates were pooled and heated

at 65°C overnight to reverse the formaldehyde cross-linking. DNA fragments were purified with a QIAquick Spin Kit (Qiagen, Valencia, CA, USA). For PCR, 1µl of purified DNA and a set of primers, corresponding to a 80 bp fragment of SNAIL1 promoter, were used by Real Time PCR.

Statistical analysis. Data are presented as means ± SD from at least three independent experiments. Statistical analysis of the data was performed by Student's *t* test. *P* values of ≤0.05 were considered statistically significant.

4. RESULTS

4.1. INDUCTION OF ROS BY TGβ1 IS ESSENTIAL FOR TRIGGERING THE EMT PROGRAM

TGF-β1-induced ROS in MCF-10A human mammary epithelial cells peak at 30-45 min and decrease thereafter (Fig.1A). ROS accumulation was sensitive to antioxidant treatments, such as N-acetyl cysteine (NAC) and peggylated-catalase (Fig. 1B). ROS induced by TGF-β1 are essential for the establishment of EMT, as revealed by changes in the levels of N-cadherin, α-SMA and E-cadherin in cells exposed to TGF-β1 and/or NAC (Fig. 1C). Confocal microscopy of E-cadherin distribution shows that scavenging of ROS by NAC inhibits TGF-β1–induced EMT. Indeed, TGF-β1 treated cells are more dispersed, show a mesenchymal like elongated spindle-shaped morphology, display well-organized actin stress fibers and reduced levels of E-cadherin (Fig. 1D, 1E).

Antioxidant (NAC) treatment inhibits the acquisition of these features confirming that in MCF10A-cells EMT induction by TGFβ1 is strictly redox-dependent. (FIG.1E.)

Determination by qPCR of *SNAIL1* mRNA, after TGF-β1 treatment, confirms its induction by TGF-β1 (Fig. 1F). The pattern of induction of *SNAIL1* by TGF-β1 is biphasic with peaks at 30 and 90 min (Fig. S1). ROS induced by TGF-β1 are essentially produced by NADPH oxidase(s)[94] and this is the reason why it has been measured *SNAIL1* induction by TGF-β1 in the presence of the general NADPH oxidase inhibitor, DPI. Under these conditions, NAC, not DPI, inhibited TGF-β1-induced *SNAIL1* gene expression, suggesting that ROS, required for the induction of *SNAIL1,* were not generated by NADPH oxidase (Fig. 1F).

4.2 Nuclear ROS and the histone demethylase, LSD1, are required for EMT induction by TGF-β1.

To find the source of ROS required for TGF-β1-induction of *SNAIL1* gene, the attention has been focused on the nucleus. A different approach has been evaluated instead of measuring nuclear ROS: these ROS are extremely unstable and may diffuse from perinuclear mitochondria, so it has been determined the accumulation of the major DNA oxidation product, 8-oxo-guanosine (8-oxoG). The Fig.2A shows a significant accumulation of 8-oxoG after 30 min of TGF-β1, in concomitance with the increase of ROS levels (Fig.1A) and EMT engagement (Fig.1C). Again, NAC inhibited 8-oxoG levels induced by TGF-β1, while DPI treatment was unable to reduce nuclear 8-oxoG induced by TGF-β1, confirming the notion that ROS were not produced by NADPH oxidases (Fig.2A).

A nuclear enzyme involved in histone demethylation and generating hydrogen peroxide, is the lysine demethylase-1, LSD1. Since LSD1 has also been associated with EMT engagement and *SNAIL1* induced repression of epithelial markers[95,96], this enzyme could be involved in the redox dependence of TGF-β1-induced EMT and DNA oxidation.

To this end, LSD1 has been silenced in MCF10A cells by shRNA-interference (Fig. 2B and S2) and 8-oxoG has been assayed upon TGF-β1 stimulation. LSD1 silencing is as effective as NAC in inhibiting DNA oxidation upon TGF-β1 stimulation (Fig. 2C), suggesting that this enzyme is the source of nuclear ROS and the cause of DNA oxidation. Then, it has been analyzed EMT engagement in MCF10A cells upon LSD1 depletion. Confocal analysis of distribution of cortical E-cadherin and formation of actin stress fibers, confirms that silencing of LSD1 inhibits EMT induced by TGF-β1 (Fig. 2D)

4.3 LSD1 down-regulates *SNAIL1* gene expression.

LSD1 is required for SNAIL1-mediated transcriptional repression[97] but it is not known if LSD1 impacts directly on *SNAIL1* expression. To find out, *SNAIL1* mRNA has been measured by qPCR in MCF10A cells depleted of LSD1. Fig.3A shows that depletion of LSD1 increases the basal expression of the gene, suggesting that LSD1 is required to maintain low SNAIL1 levels in untreated cells. To confirm the silencing of *SNAIL1* induced by LSD1, three versions of LSD1 protein has been ectopically expressed: wild type LSD1, mutALA, which encodes for an alanine NH terminal mutant of LSD1 endowed with dominant negative characteristics[98,99,100] and mutASP, which contains the same site converted into phospho-mimetic site, aspartic acid (Fig 3B). As shown in Fig. 3C and D, wild type LSD1 and the dominant negative mutant (mutALA) inhibited or enhanced *SNAIL1* basal expression, respectively. Instead, the phosphor-mimetic mutant displayed little effects on the basal, but strongly inhibited *SNAIL1* induced by TGF-β, thereby endorsing a repressor role of LSD1 in *SNAIL1* expression (Fig 3D).

4.4 LSD1: dual role in repression and induction of TGFβ1 target genes.

The data shown above do not clarify the mechanism of TGF-β1 induction of EMT, which is dependent on LSD1 generated ROS. The main apparently contradiction is how LSD1 inhibition of SNAIL1 expression can induce EMT, which is SNAIL1 dependent. It is possible that LSD1 induced ROS are required for both SNAIL1 repression and induction. LSD1 has been initially isolated from a repressor complex[101], which may mediate the silencing of SNAIL1 in unstimulated cells. Upon

TGF-β1 stimulation, LSD1 may dissociate from the repressor facilitating the formation of the transcription initiation complex. Instead, genes repressed by TGF-β1 may use LSD1 as a stable repressor. To determine if LSD1 is operating also on genes silenced by TGF-β1, WIF1, an inhibitor of EMT, has been analyzed.

TGF-β1 inhibits WIF1 expression and this effect is also mediated by LSD1, because LSD1 depletion rescues WIF1 expression in cells exposed to TGF-β1 (Fig. S3A, B). To test whether LSD1 activity was necessary for WIF1 TGF-β1 repression, cells have been pretreated with a mono-amino-oxidase inhibitor, tranylcypromine and measured the induction of SNAIL1 or the repression of WIF1 by TGF-β1. Figures S4A, B and C show that basal mRNA and protein levels of both genes increased and that SNAIL1 mRNA induction by TGF-β1 was severely impaired. WIF1 mRNA levels were higher than in the control, but still sensitive to TGF-β1 repression. These data suggest that the physical presence of active LSD1 at SNAIL1 or WIF1 promoter sites reduces basal transcription of both genes and sensitizes cells to TGF-β1 (Fig.S4). To determine the mechanism of LSD1 activation or repression of TGF-β1 target genes, following chromatin markers at the *SNAIL1* and *WIF1* promoters in cells exposed 30-60-90 min to TGFβ−1 has been analyzed: methylation of histone H3 at lysines 4 or 9 (H3k4me2-3 orH3k9me2-3); recruitment of LSD1 and JMJD2A that is a di-oxygenase, which uses a Fe++ and a coupled decarboxylation reaction to remove the repressive marks H3k9me2 or me3, which cannot be demethylated by LSD1[102]; recruitment of the co-repressor NCoR1 and HDAC3, key components of the repressor complex interacting with LSD1[103]; accumulation of OGG1 and APE1, BER enzymes that recognize 8-OxoG and abasic sites[104].

4.5 Chromatin changes induced by TGF-β1 at WIF1 and SNAIL promoters.

TGFβ1 stimulation induced significant modification of the chromatin encompassing the SNAIL1 promoter**.** The prominent changes induced by TGFβ1 at this site were: redistribution of nucleosomes with H3 depletion at 60 min (Fig.4A); late (60-90 min) methylation of H3k4me3 which is an activation mark (Fig. 4B); early (30-60 min) methylation of H3k9me2-me3 which is a repressive mark (Fig. 4C). These changes were specific to SNAIL1 promoter and were not found in other non TGFβ1 regulated genes(Fig.S5). LSD1, recruited at the promoter site in not stimulated cells, progressively decreased following TGF-β1 exposure (30–60 min) and was substituted by JMJD2A (60 min) (Fig. 4D). To link these chromatin changes to the oxidation burst induced by TGFβ1 (Fig.2A and 2C), it has been measured the recruitment of OGG1 and APE1, the BER enzymes that recognize, OGG1, and process, APE1, the oxidized site. Fig. S6A shows that OGG1 was recruited at the SNAIL1 promoter at 30 and 90 min TGF-β1 mirroring the 8-oxoG burst shown in Fig.2A. APE1, on the other hand, accumulated at SNAIL1 promoters after 90 min TGF-β1 (Fig.S6A and B). These changes were selectively induced by TGF-β1 and did not occur in other non TGFβ1 sensitive genes (Fig.S6C). Since LSD1 depletion inhibits ROS production and EMT induced by TGF-β1 (Fig. 2C-2D) and both LSD1 and JMJD2A are recruited at *SNAIL1* promoter chromatin at 30 and 90 min TGF-β1, it is likely that also JMJD2A contributes to ROS production and EMT. To find out, JMJD2A expression has been silenced in cells exposed to TGF-β1 and measured 8-oxoG and EMT. Fig.S7 shows that JMJD2A does not contribute to ROS production (Fig.S7A, B) but is essential for EMT (Fig.S7C, D, E). At *WIF1* promoter TGF-β1 induces specific changes of the histone H3 methylation code and of the other chromatin markers: H3 loss suggests a major nucleosome reorganization at 30 min TGF-β1, instead of 60 min as at *SNAIL1* promoter (Fig.5A); H3k4me2-me3, activation marks, were barely

modified by TGF-β1 (Fig. 5B); there was a peak of H3-k9 methylation 30 min following TGF-β1 exposure, overlapping with H3 loss (Fig. 5C); LSD1 accumulated steadily, while JMJD2A after an initial rise, almost disappeared at 90 min (Fig. 5D); OGG1 and APE1 accumulated at *WIF1* promoter 30-90 min, OGG1, and 30 min, APE1, after TGF-β1 stimulation (Fig.S6B).

To complete the description of histone H3 methylation changes induced by TGF-β1, the recruitment of other two H3k4 and H3k9 methylating enzymes have been monitored, SET9[105] and SUV39[106]. SET9, the H3K4me2 methyltransferase, appeared very late at the *WIF1* promoter (Fig.S8B) and very early, 30 min, at *SNAIL1* promoter (Fig.S8A), while SUV39, associated with the repressive marker, H3k9m3m, peaked at 30 min TGF-β1 at both promoters (Fig. S8A and B). The high levels at 30 min of SET9 at the *SNAIL1* promoter (Fig.S8A) were not associated with a significant increase of H3k4me2-me3, which appeared only at 90 min after TGF-β1 (Fig.4B. It may be possible that at 30 min after TGF-β1, LSD1 concentration at the promoter site is high enough to de-methylate H3k4me1 and me2, to oxidize the DNA (Fig. S6) and to compete with re-methylation of H3k4me2 by SET9 action. A further reduction of LSD1 at this site (60-90 min TGF-β1) leads to a substantial methylation of H3k4me2 and accumulation of H3k4me3 (Fig.4B).

4.6 TGF-β 1 induced-phospho-SMAD2/3 recruits JMJD2A and promotes LSD1 depletion at the *SNAIL1* promoter.

The changes of the histone H3 methylation and LSD1-JMJD2A levels, recruited at TGF-β1-activated or repressed promoters, correlate well with the progressive loss or accumulation of repressors (NCoR1 and HDAC3) at the *SNAIL1* and the *WIF1* promoters, respectively (Fig.6A and B). However, these data do not clarify the initial event triggered by TGF-β1. TGF-β1 induces SMAD2-3 phosphorylation and the accumulation of these factors in the nucleus are essential for EMT induction[107]. Thus, phosphorylated SMAD2-3 steadily increases at 30 and 60 min TGF-β1 at the *SNAIL1* promoter (Fig.6C), whereas at the *WIF1* promoter accumulates essentially only the un-phosphorylated SMAD2-3 (Fig.6D). To find the partners associated with SMAD2-3, re-ChIP analysis on SMAD2-3 chromatin immuno-precipitates with antibodies against LSD1 and JMJD2A has been performed. TGF-β1 reduced SMAD2-3/LSD1 and increased SMAD2-3/ JMJD2A at *SNAIL1* promoter, (Fig.S9B and C), whereas at the *WIF1* promoter, TGF-β1 promoted the interaction of LSD1 with SMAD2-3 (Fig.S10). Taking into account that at the *SNAIL1* promoter phosphorylated SMAD2-3 were selectively recruited at 30-60 min TGF-β1 (Fig.6C) and at *WIF1* promoter were present essentially only un-phosphorylated SMAD2-3 at 30-90 min TGF-β1 (Fig.6D), it could be possible to conclude that the phosphorylation of SMAD2-3 induced by TGF-β1 is the critical event that facilitates the formation of a transcription-active (SMAD2-3/JMJD2A) or inactive (SMAD2-3/LSD1) complex at the *SNAIL1* and *WIF1* promoters, respectively (Fig.S9 and S10). To better define the interaction between SMAD2-3, LSD1 and JMJD2A, it has been performed direct immune-precipitation analysis of total cell extracts derived from cells exposed to TGF-β1. Fig. 6E and F show that TGF-β1 facilitates the interaction of SMAD2-3 with JMJD2A and reduces the complex SMAD2-3/LSD1. Although it has not been possible

to purify selectively pSMAD2-3/JMJD2A complex with the phospho-SMAD-specific antibodies, we suggest that the switch at the *SNAIL1* promoter of SMAD2-3/LSD1 to SMAD2-3/JMJD2A is favored by higher concentrations of phosphoSMAD2-3 at this site induced by TGF-β1(Fig.6C).

4.7 TGFβ transiently reduces LSD1 protein levels

Another possibility that might explain the loss of LSD1 and the increase of JMJD2A at *SNAIL1* promoter induced by TGF-β1 is the change of protein levels of the two enzymes. While it is well established that pSMAD2-3 are induced by TGF-β1 (34), it is unknown if TGF-β1 has any effect on LSD1 or JMJD2A protein levels. To this end, it has been measured the concentration of these proteins in TGF-β1-induced cells. Figures S11A-B show that LSD1 protein levels, not JMJD2A, were reduced in TGF-β1 exposed cells, although at 90 min, TGF-β1 did not modify LSD1 mRNA levels (Fig.S2). This reduction is likely due to proteasome activation by the cytokine, since MG132, a cell-permeable proteasome inhibitor, prevented the drop of LSD1 levels (Figures S11C and D). Reduction of LSD1 protein attenuates nuclear ROS levels (Fig.2A), but does not affect LSD1 mRNA (Fig.S2) or LSD1 associated with other repressors at other sites (Fig.5D). Lower LSD1 concentrations shift the binding of pSMAD2-3 to JMJD2A, which levels remain constant in TGF-β1-exposed cells (Fig.S11B). Figure 7 shows a summary of the chromatin changes at *SNAIL1* and *WIF1* promoters in cells exposed to TGF-β1. The growth factor induces changes of histone (H3) methylation code and recruitment of various factors to the *SNAIL1* and *WIF1* promoters. Specifically all profiles shown, display a biphasic pattern and that the period 30 to 60 min of TGF-β1 stimulation is critical for the activation of *SNAIL1* and repression of *WIF1*. This is suggested by the following observations: the histone H3 eviction is very rapid (30 min) and overlaps with high LSD1 levels at

WIF1 promoter (Fig.5D); at the *SNAIL1* site, the repressive complex is eliminated stepwise, first, HDAC3 at 30 min, second, LSD1 at 60 min and eventually, NCoR1 at 90 min (Fig.4D and 6A); between 30 and 60 min, pSMAD2-3 and JMJD2A form a complex at the *SNAIL1* promoter site (Fig.S9A); at 60 min, OGG1 levels, present at *SNAIL1* and *WIF1* promoter sites, significantly decrease (Fig.S6) as well as the levels of histone methyltransferases, SUV39 and SET9 (Fig.S8A); at 90 min TGF-β1, LSD1 is again recruited at the *SNAIL1* promoter, but without the co-repressor NCOR1 or HDAC3 (Fig. 4D and 6A). In the absence of repressors, LSD1, *in vivo* can demethylases H3k9me2 and activate transcription (Fig.4D)[108,109,110]. Collectively, Fig.7 shows that histone methylation-demethylation, recruitment of repair enzymes and transcription factors (pSMAD2-3) follow a cyclical pattern both at the TGF-β1-induced (*SNAIL1*) or repressed (*WIF1*) transcription units. These chromatin changes are similar to those observed in cells constitutively expressing *SNAIL1* gene[111]. The critical event is the appearance of phospho-SMAD2-3 at the *SNAIL1* promoter. At this site, the phosphorylated proteins stabilize the active complex formed with JMJD2A (Fig.S9). These sites are previously cleared by LSD1, which reduces the basal transcription and sensitizes the cells to TGF-β1. Only under these conditions it has been possible to detect TGF-β1-induced early chromatin and transcriptional changes. After 90 min TGF-β1 exposed cells de-synchronize and the cyclical chromatin changes escape detection due to increased cell-to-cell stochastic variations[112,113,114].

5.DISCUSSION

The data reported show that in epithelial mammary cells, EMT induced by TGFβ1 is a redox dependent process. Many studies in the last years have been focused their attention on the role of ROS in EMT [115,116]. Oxidative stress is a complex process implicated in many human pathological and physiological pathways. Many factors such as inflammation, cytokines, grow factors produced and released in tumors microenvironment by various cell types such as cancer associated fibroblast, CAF, or macrophages may cause oxidative stress in epithelial cells which can sustain EMT program. With this work, an important element is added: ROS induced by TGF-β1 in the nuclear compartment by the histone demethylase, LSD1, are essential for SNAIL1 induction and the establishment of the EMT program.

5.1 Nuclear ROS wave induced by TGF-β1

It's well known that TGFβ1 induces an initial oxidation, generated by membrane-bound NADPH oxidase enzymes which are NOX-2 and NOX-4[117]. This is accompanied by activation of SMADs proteins, which are phosphorylated by several kinases, including stress kinases, JNK, p38. While this membrane-cytosolic pattern is well known[118], nuclear oxidation burst TGβ1 induced is novel. The source of these nuclear ROS is the histone demethylase LSD1 (Fig. 2C) and nuclear ROS production causes DNA oxidation testified by recruitment of OGG1 at the *SNAIL1* or *WIF1* promoters; a recruitment that suggests an activation and a repression of transcription by TGF-β1, mediated by ROS. Changes of histone methylation code and loss or gain of repressors correlate very well with activation of *SNAIL1* and repression of *WIF1* transcription induced by TGF-β1.

5.2 TGF-β1 coordinates the action of LSD1 and JMJD2A to induce SNAIL1 expression

Timing in TGFβ1 induced EMT is very important, since the main chromatin changes occurs within 30-60 minutes after TGβ1 administration (Fig.7). Indeed TGβ1 at 30 minutes, facilitates the recruitment of JMJD2A and the successive elimination of H3-k9me3, a repressive marker, at 60 minutes at SNAIL1 promoter (FIG.4C and 4D). On the other hand, *WIF1* promoter is stably silenced by the recruitment of LSD1 (Fig.5D) and associated co-repressors (NCoR1-HDAC3) (Fig. 6B).

TGF-β1-induced LSD1, transiently represses *SNAIL1* and prepares the promoter for the activation by JMJD2A (Fig.4). Conversely, the significant gain of repressors at *WIF1* promoter (30-60 min TGF-β1) induces stable repression of transcription (Fig.6). These date show the poliedric effect of a signal, which could induce both transient and stable repression depending on factors recruited at promoters sites.

It is important to underline that activation of SNAIL1 requires both LSD1 and JMJD2A: basal transcription of SNAIL1 is turned off by cooperation of LSD1 together with NCor1 and HDAC3 (Fig.4D and 6A) which physically occupy SNAIL1 promoter. After TGFβ1 treatment, LSD1 further reduces basal transcription by demethylating H3K4me2, an active marker, but at 60 minutes the enzyme is turned away from SNAIL1 promoter by a complex formed by pSMAD and JMJD2A (Fig.6C and D). LSD1 demethylates H3k4me2, which is formed by SET9, recruited at 30 min at the *SNAIL1* promoter (Fig.7). The other histone demethylase JMJD2A, upon TGF-β1 challenge, demethylates H3k9me3, a repressive marker, (Fig.4C) and activates transcription associated with pSMAD2/3 (Fig.6C). The oxidation burst at 30 minutes is due to cells synchronization by TGFβ1 as shown by 8-oxoG signal (Fig. 2) and to LSD1 activity but not JMJD2A (Fig.S7). The importance of the presence of LSD1 at the SNAIL1 promoter to trigger EMT has been shown by LSD1 depletion or expression

of LSD1 dominant negative mutant: high levels of basal SNAIL1 block EMT induced by TGFβ1 (FIG. 2). Moreover, LSD1, in the absence of JMJD2A, cannot induce TGFβ1 EMT (Fig. S7) indicating that LSD1 cooperates with JMJD demethylases. Members of JMJD family required for EMT TGF-β1 induced are known. For example, JMJD3, which demethylates H3k27m3, another repressive mark, is required for EMT induction[119]. Collectively, these data highlight the role of JMJD demethylases and their cooperation with LSD1 to induce EMT. There is also a general implication on the control of nuclear oxidation. These enzymes with a different mechanism of action control both hydrogen peroxide levels (LSD1) and redox status of iron since JMJD family enzymes contain Fe++. This control of DNA oxidation represents an important factor assisting the recruitment and the assembly of transcription initiation complex that triggers EMT.

5.3 Periodic cycles of histone methylation and DNA oxidation, induced by TGβ1, govern the induction of EMT transcriptional program.

This process which opens the chromatin, induces formation of chromatin loops and governs cycles of histone methylation, is very similar to the events induced by estrogens and retinoic acid to stimulate transcription of target genes [120,121,122].
Simultaneously to this, WIF1 silencing by TGβ1 occurs through complex constituted by LSD1-HDAC3-NCor1 (Fig. 6B and Fig. S3). Moreover, also in this process, ROS play a fundamental role involving other factors such as JNK and ATF3[123]. The final result is the inhibition of WIF and activation of Wnt/β-catenin cascade, which contributes to EMT program.
Summarizing, EMT program could be described as an oscillatory process where transient and reversible changes of chromatin could reflect typical features of EMT

such as reversibility and gradient of intermediate expression between epithelial and mesenchymal state. These changes, responsible for activation or suppression of transcription, occur in a specific time frame where LSD1, stimulated by TGFβ1, takes on the role of metronome.

6.FIGURES AND TABLES

Figure 1

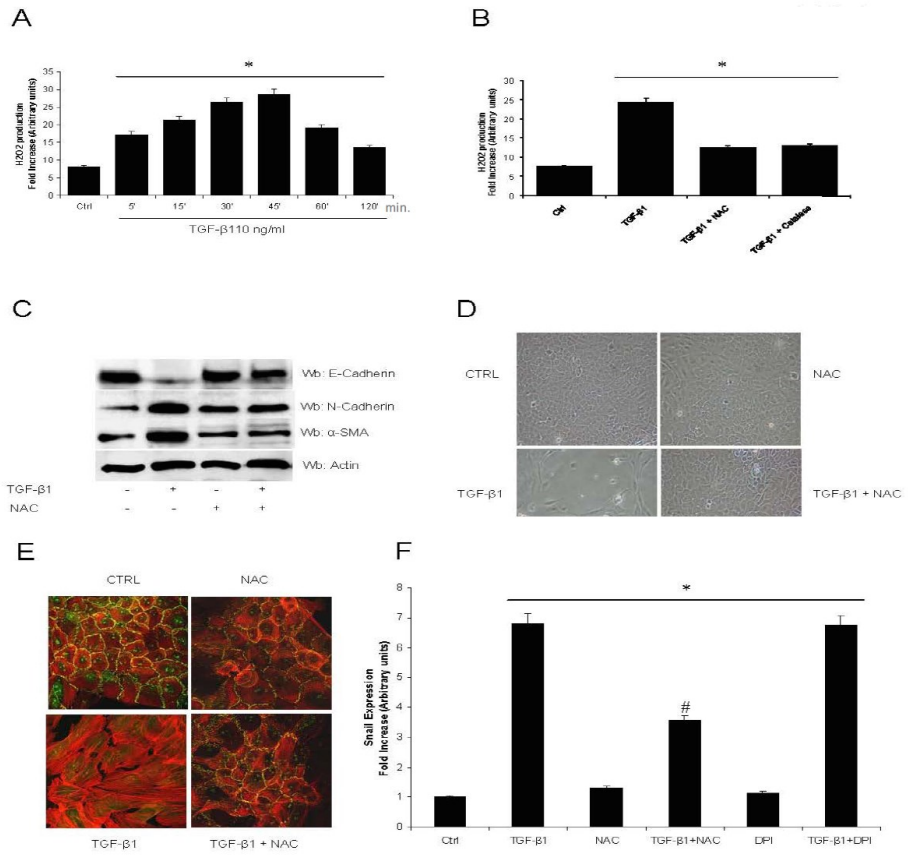

Figure 2

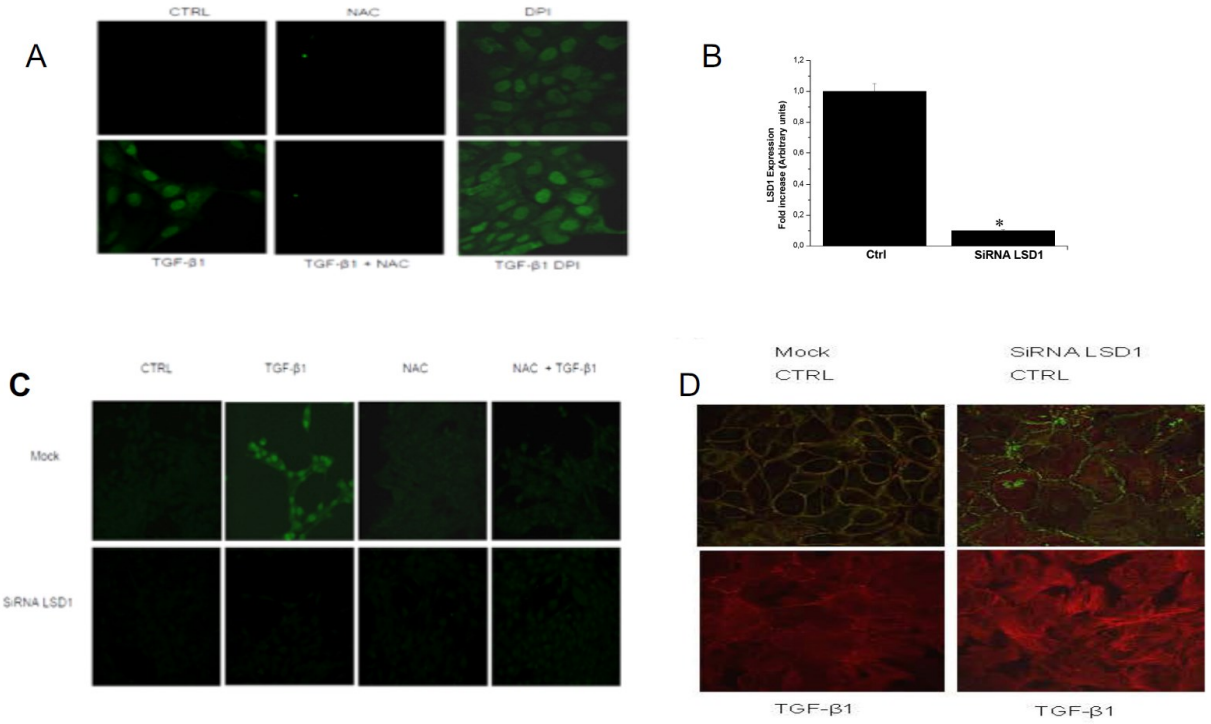
A
CTRL
NAC
DPI
TGF-β1
TGF-β1 + NAC
TGF-β1 DPI
B
LSD1 Expression
Fold increase (Arbitrary units)
1,2
1,0
0,8
0,6
0,4
0,2
0,0
*
Ctrl
SiRNA LSD1
C
CTRL
TGF-β1
NAC
NAC + TGF-β1
Mock
SiRNA LSD1
D
Mock
CTRL
SiRNA LSD1
CTRL
TGF-β1
TGF-β1

Figure 3

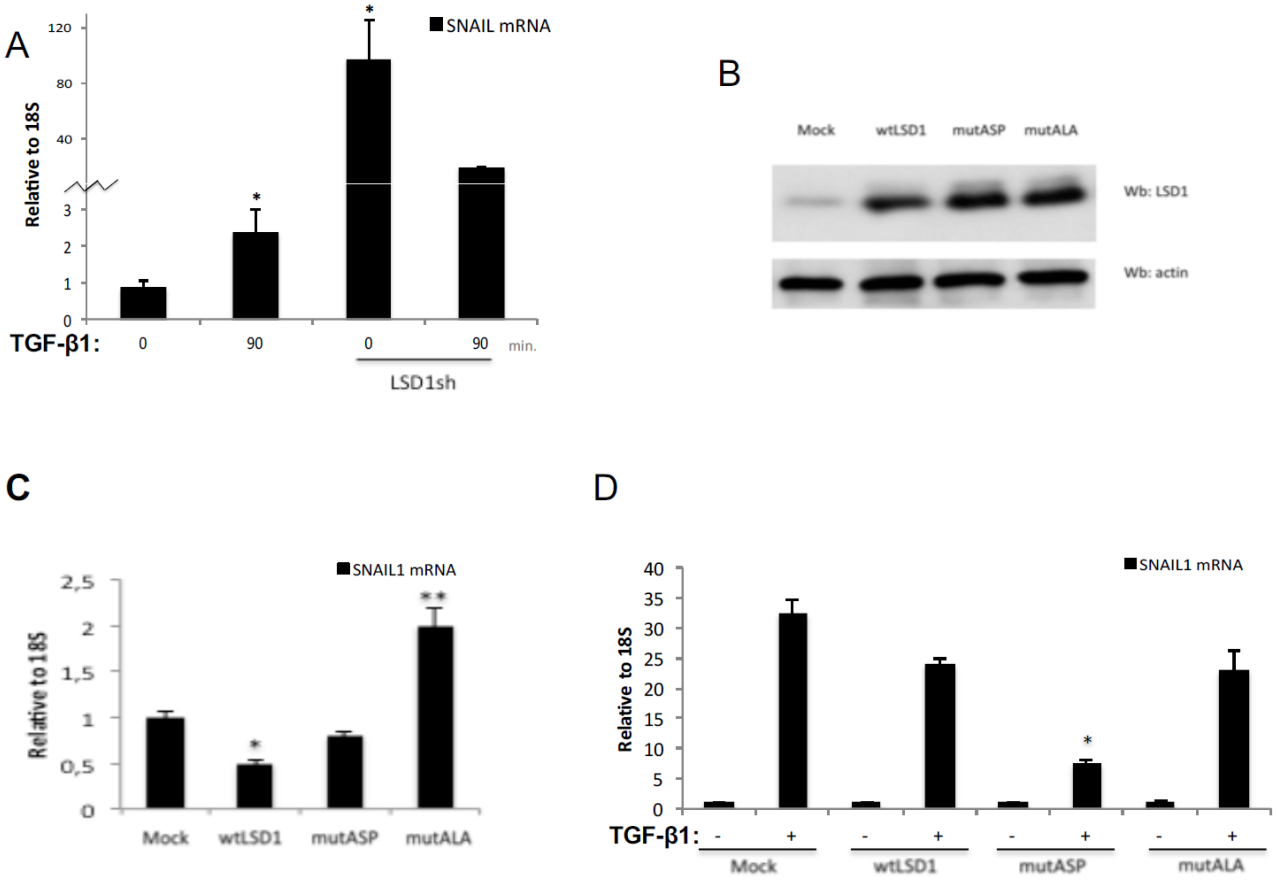
A
SNAIL mRNA
Relative to 18S
120
80
40
3
2
1
0
TGF-β1:
0
90
0
90
min.
LSD1sh
B
Mock
wtLSD1
mutASP
mutALA
Wb: LSD1
Wb: actin
C
SNAIL1 mRNA
Relative to 18S
2,5
2
1,5
1
0,5
0
Mock
wtLSD1
mutASP
mutALA
D
SNAIL1 mRNA
Relative to 18S
40
35
30
25
20
15
10
5
0
TGF-β1:
-
+
Mock
wtLSD1
mutASP
mutALA

Figure 4

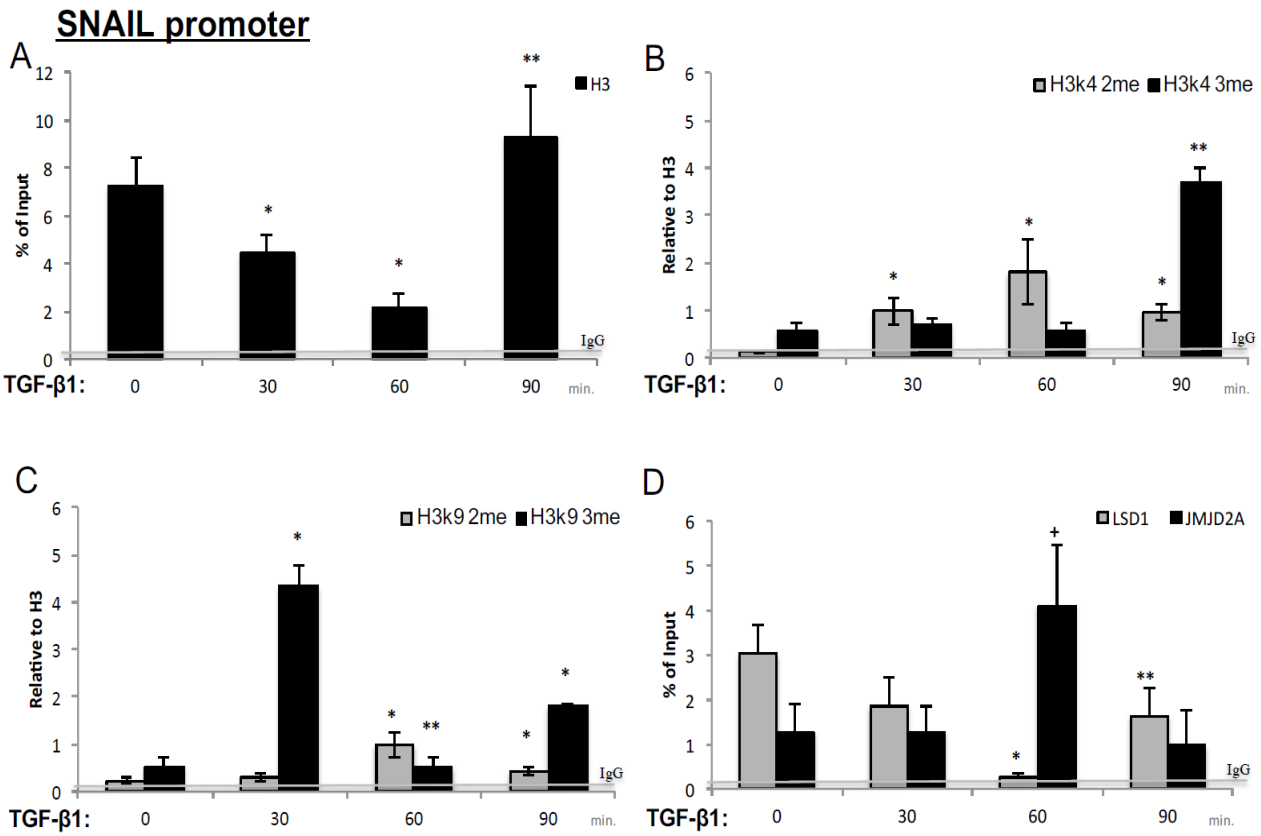
SNAIL promoter
A
% of Input
H3
IgG
TGF-β1: 0 30 60 90 min.
B
Relative to H3
H3k4 2me
H3k4 3me
IgG
TGF-β1: 0 30 60 90 min.
C
Relative to H3
H3k9 2me
H3k9 3me
IgG
TGF-β1: 0 30 60 90 min.
D
% of Input
LSD1
JMJD2A
IgG
TGF-β1: 0 30 60 90 min.

Figure 5

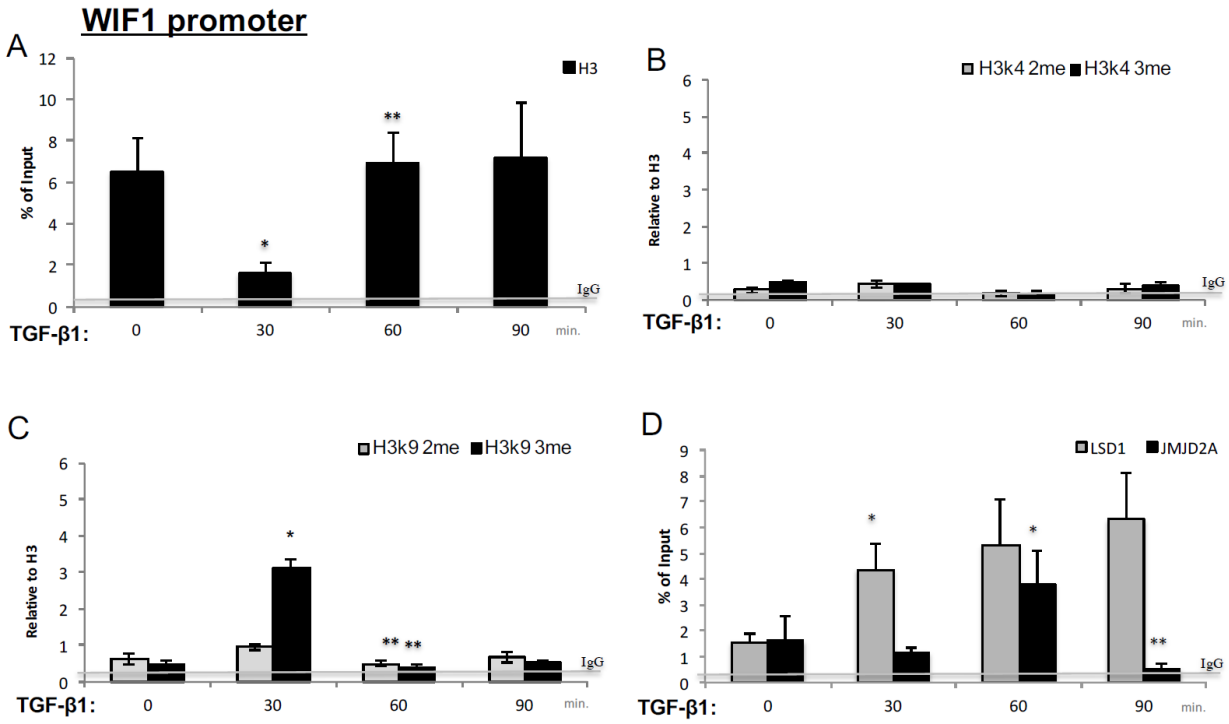
WIF1 promoter
A
H3
% of Input
IgG
TGF-β1: 0 30 60 90 min.
B
H3k4 2me H3k4 3me
Relative to H3
IgG
TGF-β1: 0 30 60 90 min.
C
H3k9 2me H3k9 3me
Relative to H3
IgG
TGF-β1: 0 30 60 90 min.
D
LSD1 JMJD2A
% of Input
IgG
TGF-β1: 0 30 60 90 min.

Figure 6

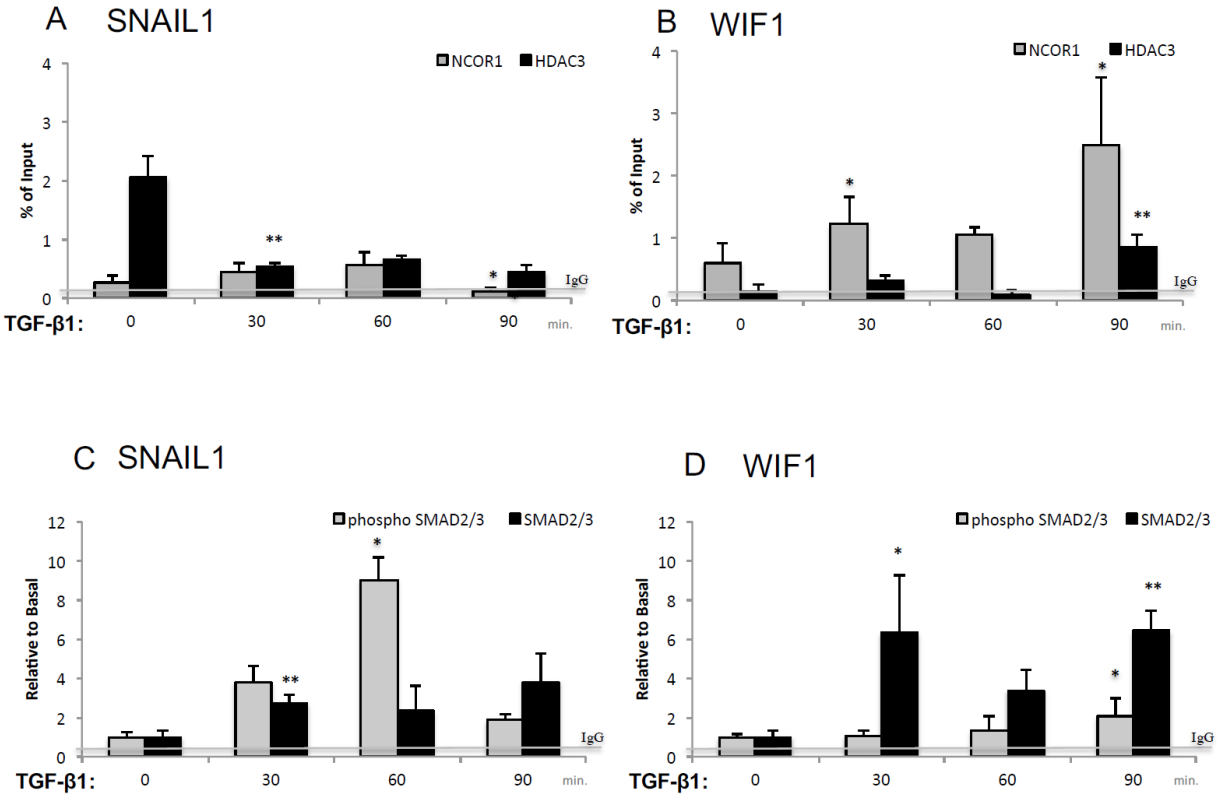

Figure 6

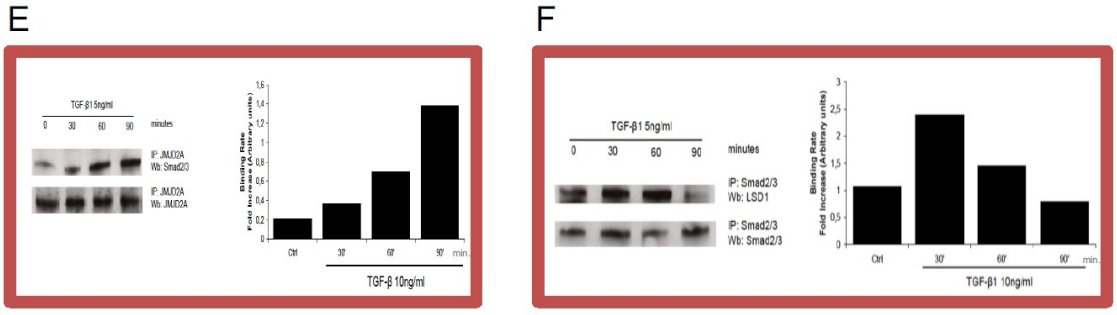

Figure 7

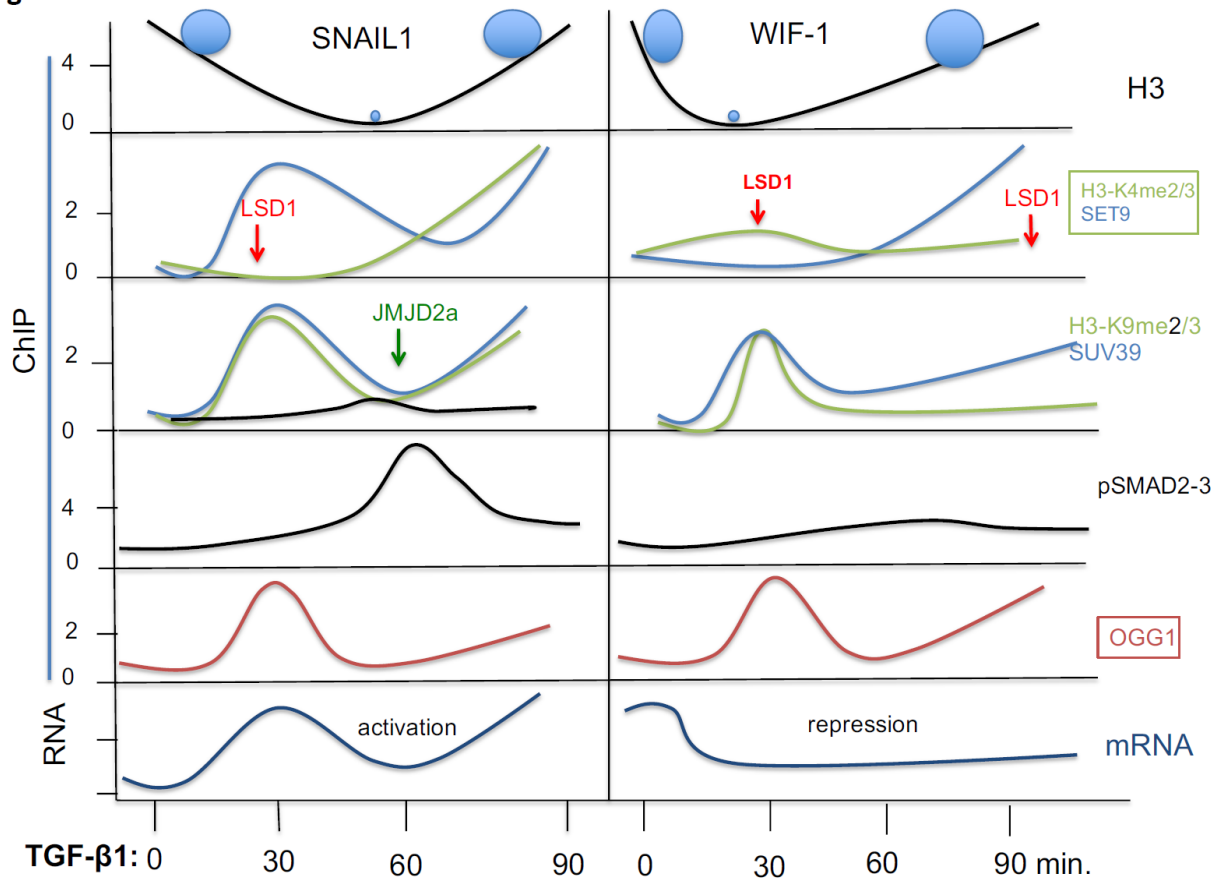
SNAIL1
WIF-1
H3
LSD1
LSD1
LSD1
H3-K4me2/3
SET9
JMJD2a
H3-K9me2/3
SUV39
pSMAD2-3
OGG1
ChIP
RNA
activation
repression
mRNA
TGF-β1: 0 30 60 90 0 30 60 90 min.

Fig.S1

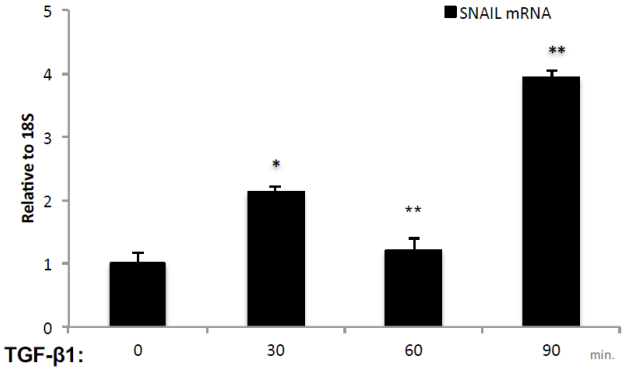
SNAIL mRNA
Relative to 18S
5
4
3
2
1
0
*
**
**
TGF-β1:
0
30
60
90
min.

Fig. S2

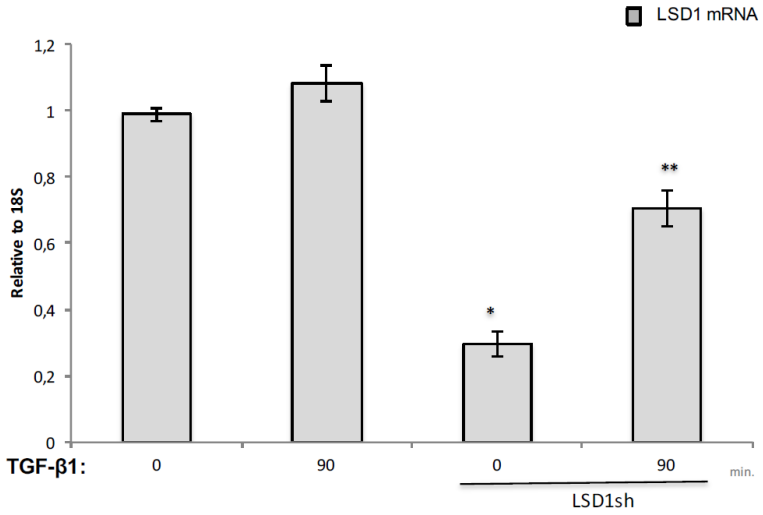
LSD1 mRNA
Relative to 18S
1,2
1
0,8
0,6
0,4
0,2
0
*
**
TGF-β1:
0
90
0
90
min.
LSD1sh

Fig. S3

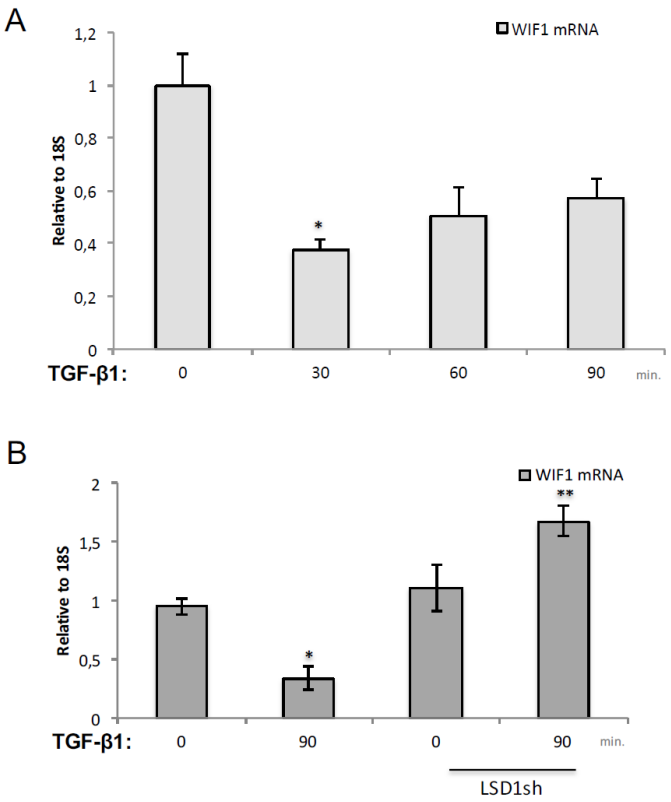
A
WIF1 mRNA
Relative to 18S
1,2
1
0,8
0,6
0,4
0,2
0
*
TGF-β1:
0
30
60
90
min.
B
WIF1 mRNA
Relative to 18S
2
1,5
1
0,5
0
*
**
TGF-β1:
0
90
0
90
min.
LSD1sh

Fig. S4

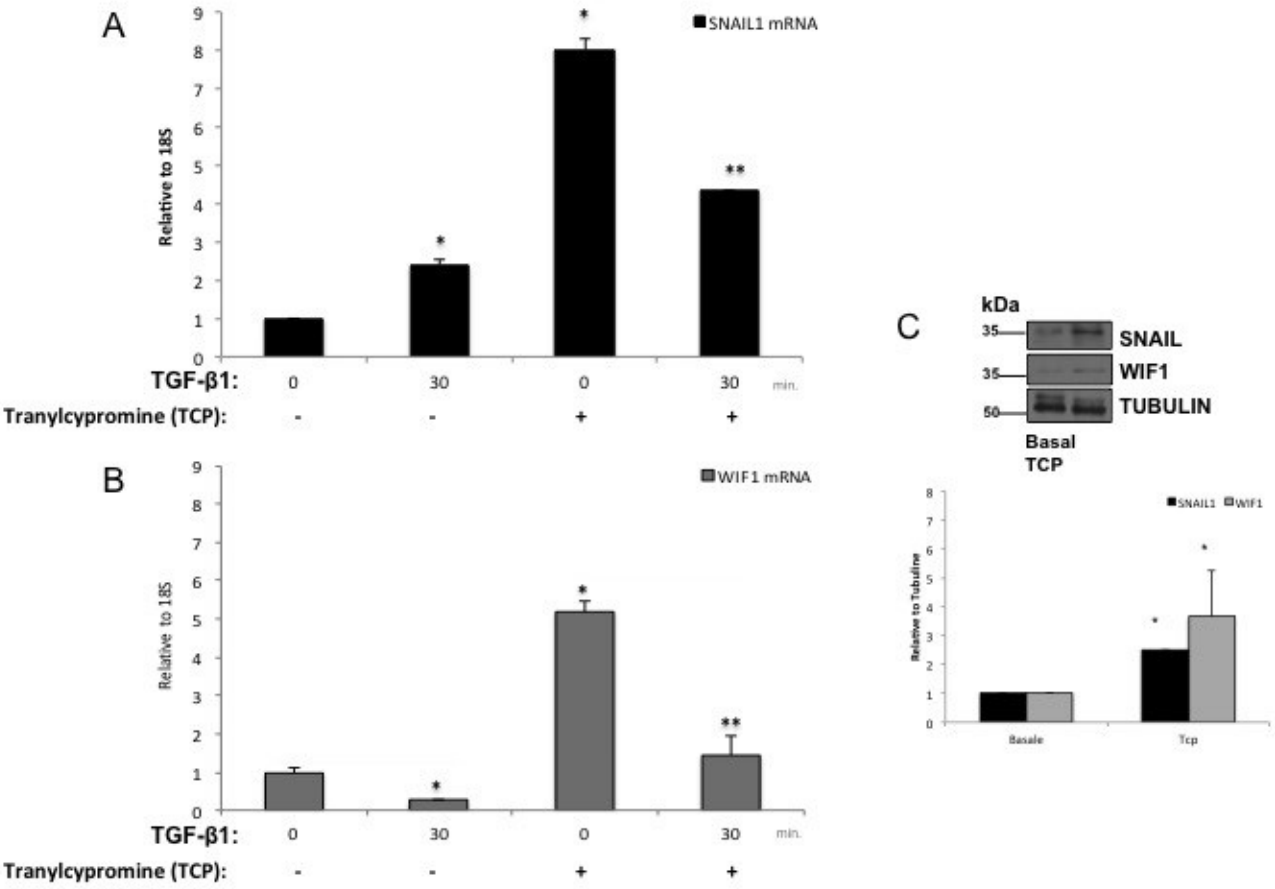
A
SNAIL1 mRNA
Relative to 18S
TGF-β1: 0 30 0 30 min.
Tranylcypromine (TCP): - - + +
B
WIF1 mRNA
Relative to 18S
TGF-β1: 0 30 0 30 min.
Tranylcypromine (TCP): - - + +
C
kDa
35 SNAIL
35 WIF1
50 TUBULIN
Basal
TCP
SNAIL1 WIF1
Relative to Tubulin
Basale
Tcp

Fig. S5

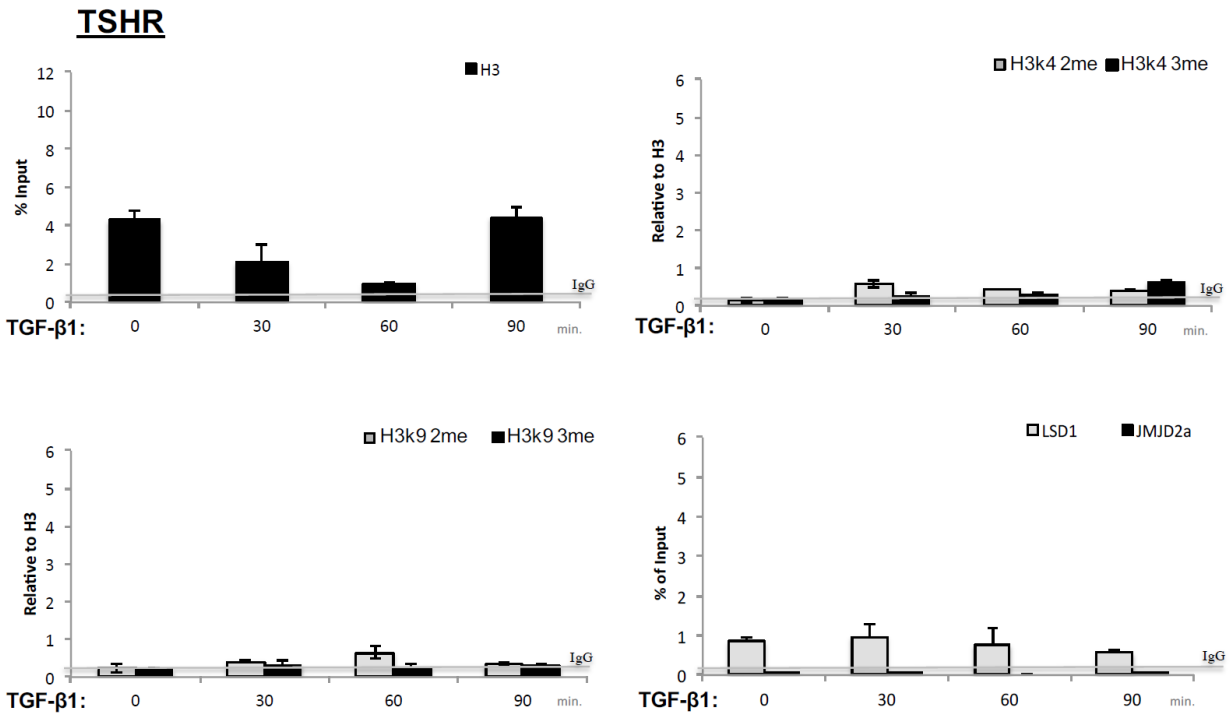
TSHR
H3
% Input
IgG
TGF-β1:
0
30
60
90
min.
H3k4 2me
H3k4 3me
Relative to H3
H3k9 2me
H3k9 3me
LSD1
JMJD2a
% of Input

Fig. S6

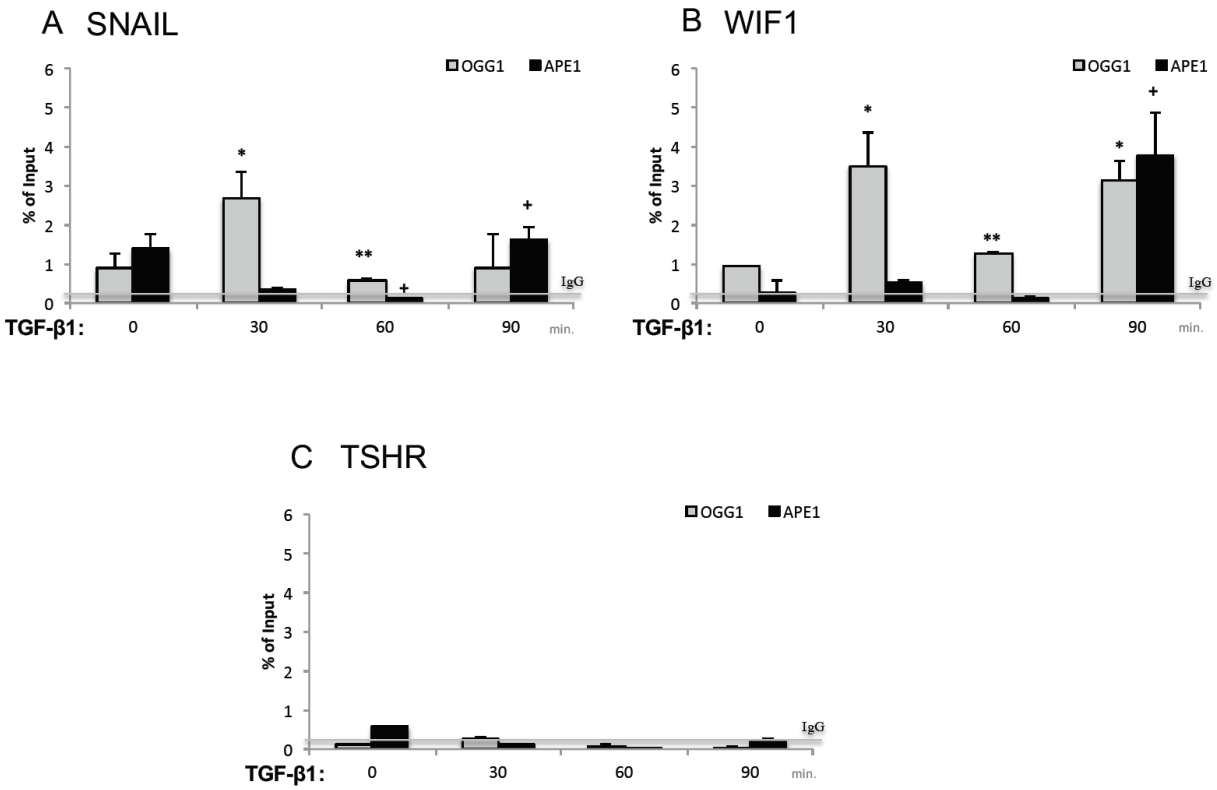
A SNAIL
OGG1
APE1
% of Input
IgG
TGF-β1:
0
30
60
90
min.
B WIF1
OGG1
APE1
% of Input
IgG
TGF-β1:
0
30
60
90
min.
C TSHR
OGG1
APE1
% of Input
IgG
TGF-β1:
0
30
60
90
min.

Fig. S7

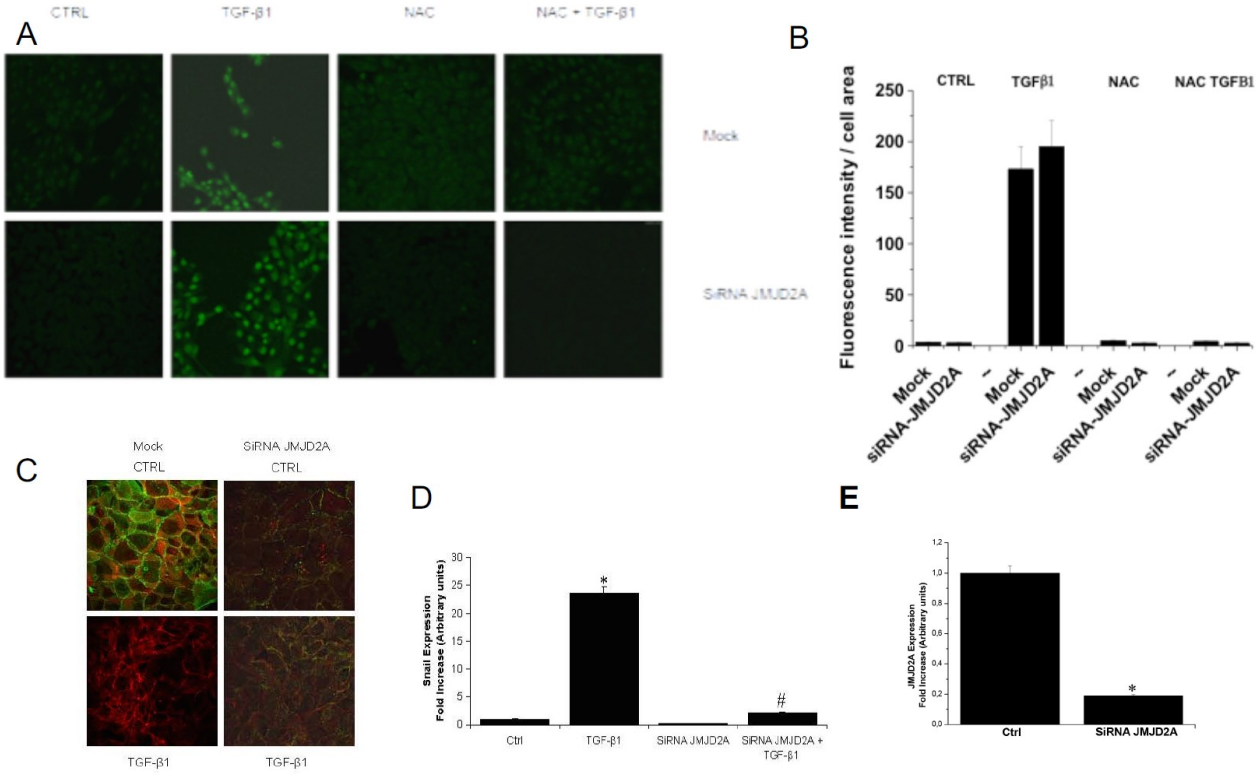
A
CTRL
TGF-β1
NAC
NAC + TGF-β1
Mock
SiRNA JMJD2A
B
CTRL
TGFβ1
NAC
NAC TGFB1
Fluorescence intensity / cell area
250
200
150
100
50
0
Mock
siRNA-JMJD2A
C
Mock
CTRL
SiRNA JMJD2A
CTRL
TGF-β1
TGF-β1
D
Snail Expression
Fold Increase (Arbitrary units)
30
25
20
15
10
5
0
*
#
Ctrl
TGF-β1
SiRNA JMJD2A
SiRNA JMJD2A + TGF-β1
E
JMJD2A Expression
Fold Increase (Arbitrary units)
1,2
1,0
0,8
0,6
0,4
0,2
0,0
*
Ctrl
SiRNA JMJD2A

Fig.S8

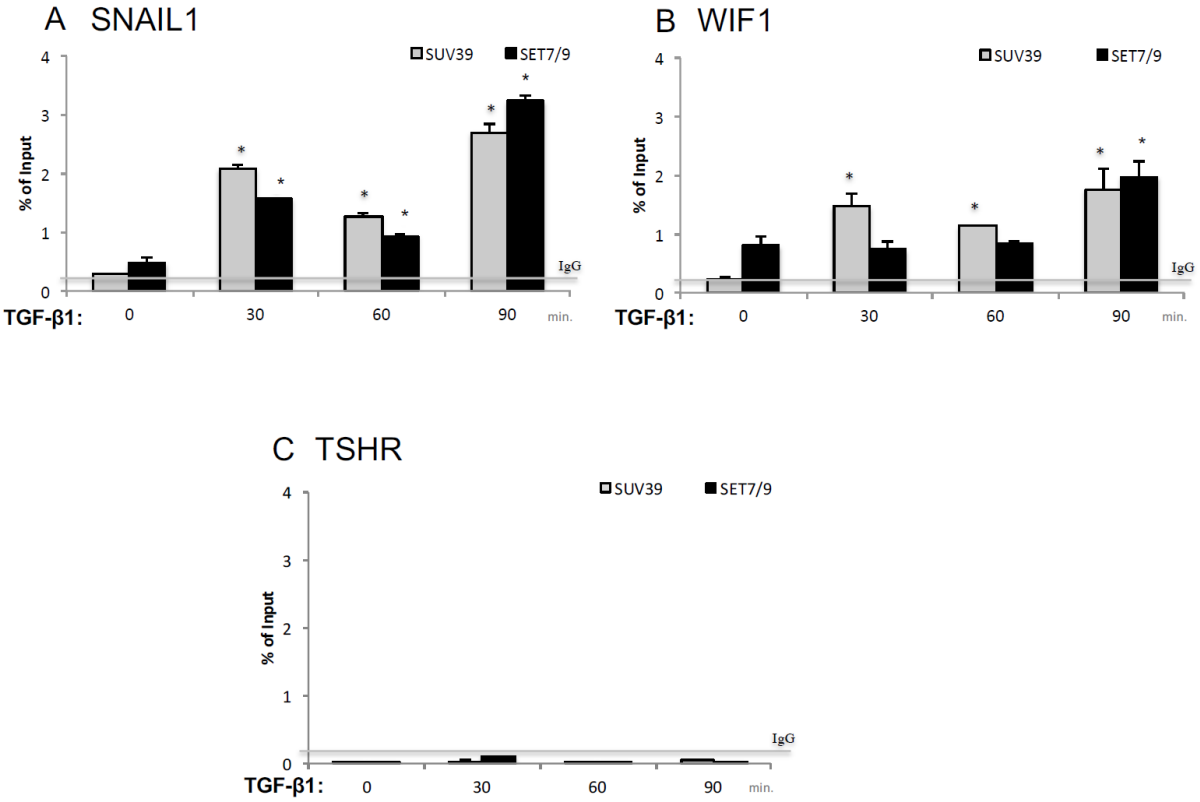
A SNAIL1
SUV39
SET7/9
% of Input
IgG
TGF-β1:
0
30
60
90
min.
B WIF1
SUV39
SET7/9
% of Input
IgG
TGF-β1:
0
30
60
90
min.
C TSHR
SUV39
SET7/9
% of Input
IgG
TGF-β1:
0
30
60
90
min.

Fig.S9

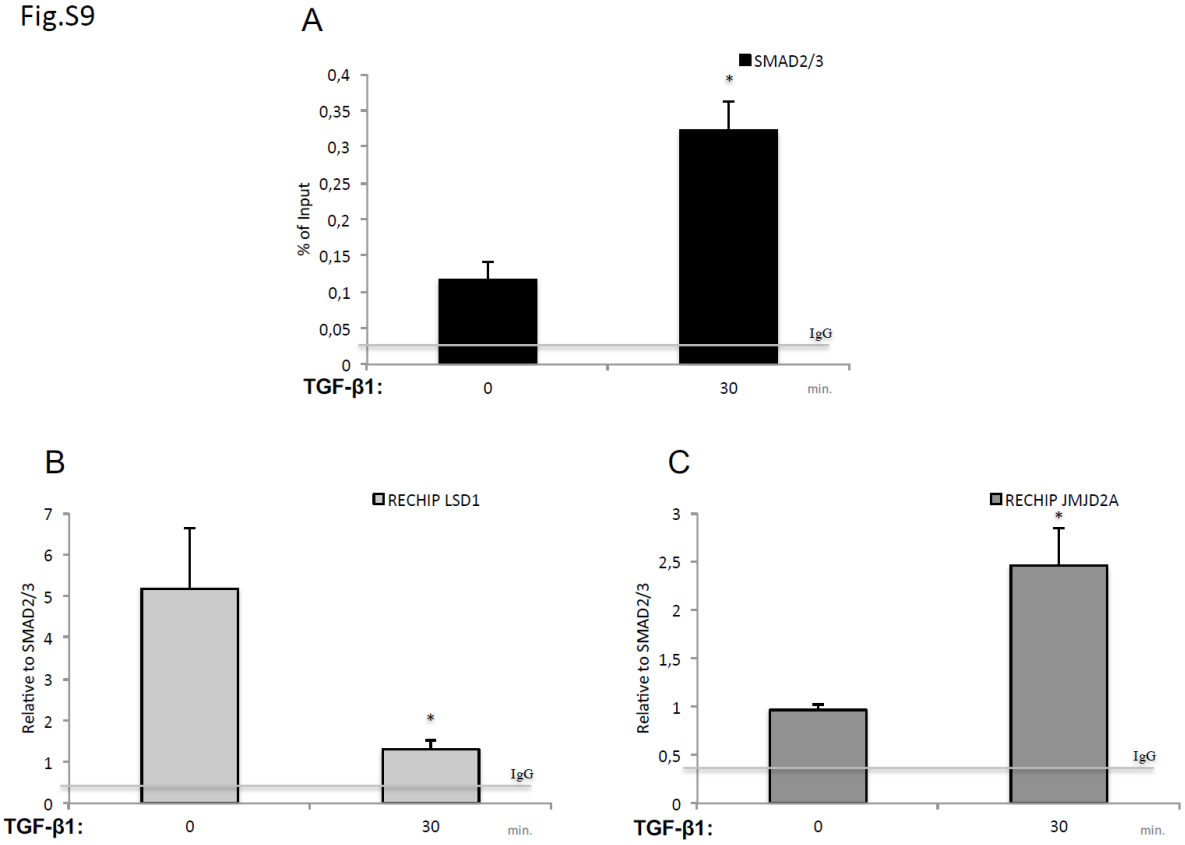
A
SMAD2/3
% of Input
0,4
0,35
0,3
0,25
0,2
0,15
0,1
0,05
0
IgG
TGF-β1:
0
30
min.
B
RECHIP LSD1
Relative to SMAD2/3
7
6
5
4
3
2
1
0
IgG
TGF-β1:
0
30
min.
C
RECHIP JMJD2A
Relative to SMAD2/3
3
2,5
2
1,5
1
0,5
0
IgG
TGF-β1:
0
30
min.

Fig.S10

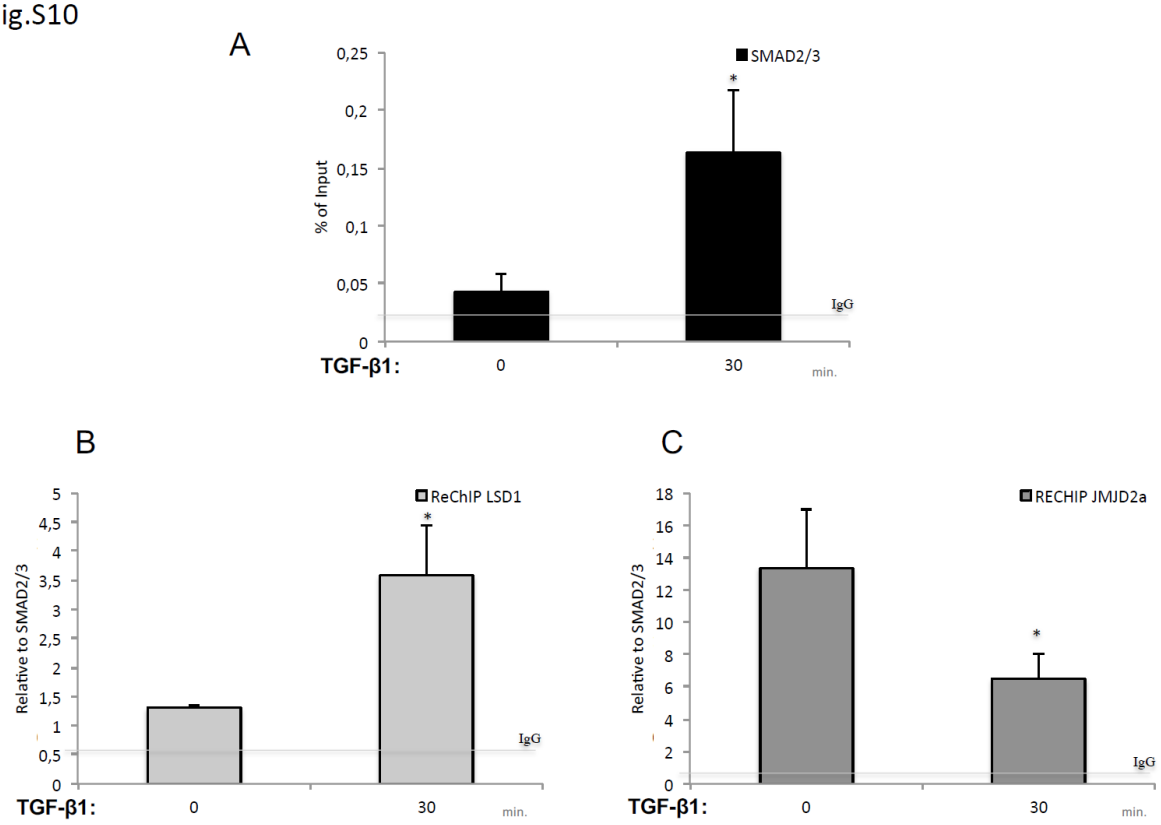
A
SMAD2/3
% of Input
0,25
0,2
0,15
0,1
0,05
0
IgG
TGF-β1:
0
30
min.
B
ReChIP LSD1
Relative to SMAD2/3
5
4,5
4
3,5
3
2,5
2
1,5
1
0,5
0
IgG
TGF-β1:
0
30
min.
C
RECHIP JMJD2a
Relative to SMAD2/3
18
16
14
12
10
8
6
4
2
0
IgG
TGF-β1:
0
30
min.

Fig. S11

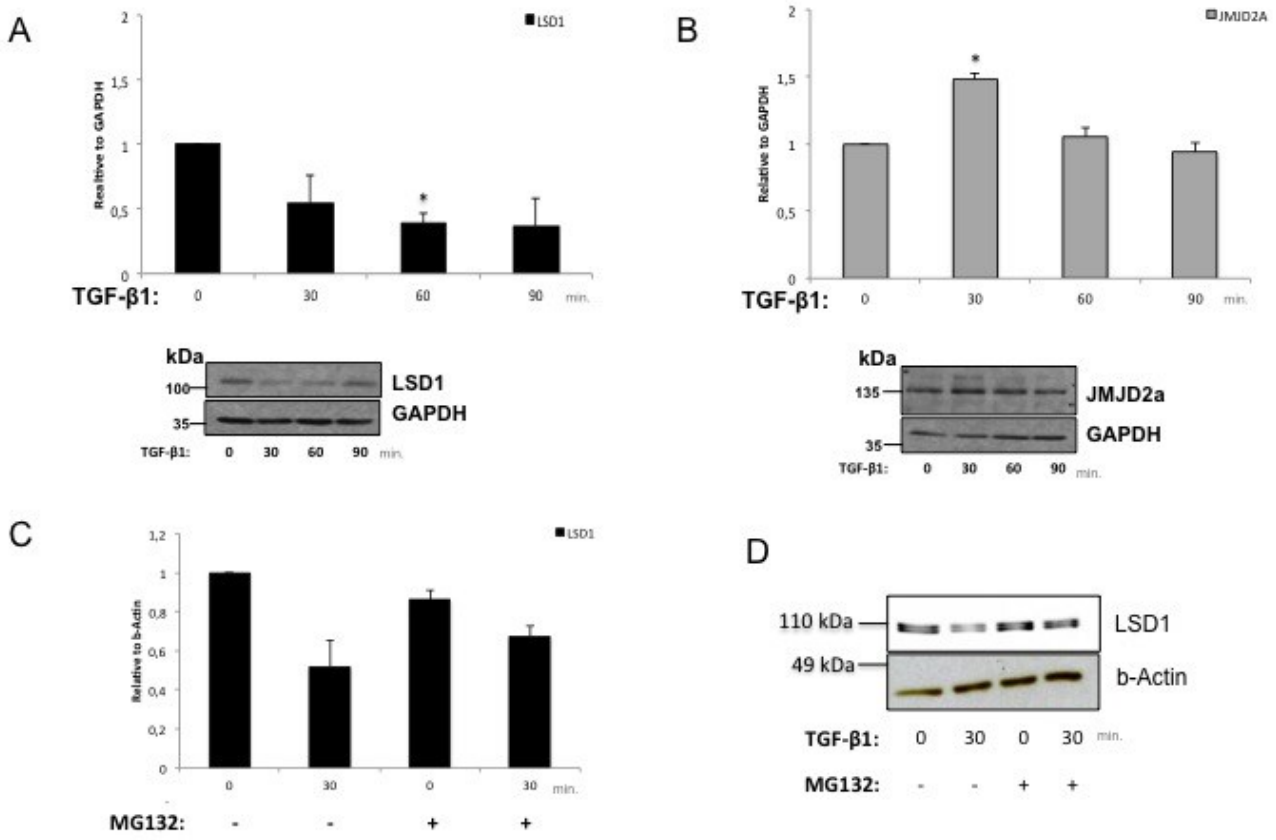
A
LSD1
Relative to GAPDH
2
1,5
1
0,5
0
*
TGF-β1: 0 30 60 90 min.
kDa
100
35
LSD1
GAPDH
TGF-β1: 0 30 60 90 min.
B
JMJD2A
Relative to GAPDH
2
1,5
1
0,5
0
*
TGF-β1: 0 30 60 90 min.
kDa
135
35
JMJD2a
GAPDH
TGF-β1: 0 30 60 90 min.
C
LSD1
Relative to b-Actin
1,2
1
0,8
0,6
0,4
0,2
0
0 30 0 30 min.
MG132: - - + +
D
110 kDa
49 kDa
LSD1
b-Actin
TGF-β1: 0 30 0 30 min.
MG132: - - + +

Table T1:

mRNA	
SNAIL Fw	*5'-GAGGCGGTGGCAGACTAG-3'*
SNAIL Rv	*5'-GACACATCGGTCAGACCAG-3'*
WIF1 Fw	*5'-TGAAGTGGATGTGATTGTTATG-3'*
WIF1 Rv	*5'-TCAGGACACTCGCAGATGCGT-3'*
LSD1 Fw	*5'-GATTCAGCTGACATTTGAGGCT-3'*
LSD1Rv	*5'-CTGTCGAGCTGCTGCCAAGCCT-3'*
JMJD2A Fw	*5'-CCAGAACCAACCAGGAGC-3'*
JMJD2A Rv	*5'-TTCACT GCGCGAGACCAT-3'*
18S Fw	*5'-GCGCTACACTGACTGGCTC-3'*
18SRv	*5'-CATCCAATCGGTAGTAGCGAC-3'*
ChIP	
SNAIL Fw	*5'-ACTGGACCAGAAGCTACCCTTCG-3'*
SNAIL Rv	*5'-TGACATCTGAGTGGGTCTG-3'*
WIF1 Fw	*5'-CGGGTTATCAGGGAGACAGA-3'*
WIF1 Rv	*5'-CTCCCTTTCAGCCAGTAGGA-3'*
TSHR Fw	*5'-ACCGAGACCCCTCTTGCTCT-3'*
TSHR Rv:	*5'-AGTTGCTAACAGTGATGAGAGGCT-3'*

6.1 FIGURE LEGENDS

Fig. 1. TGF β1-induced ROS are essential for EMT in MCF-10A cells.

A and **B:** ROS induced by TGF-β1. **A**. Cells were serum-starved for 24h before stimulation with 10 ng/ml TGF-β1 for the indicated times. H_2O_2 production was evaluated as described in Materials and Methods. The results are representative of three experiments. Student t-test, ∗p<0.005 treatments *vs* control. **B.** Cells were pretreated with 5 mM NAC or 1 μg/ml catalase for 15 min before stimulation with 10 ng/ml TGF-β1 for 30 min. The results are representative of three experiments. Student t-test, ∗p<0.005 treatments *vs* control. **C** to **F:** E-N cadherin switch induced by TGFβ1. Cells were pre-treated with 5 mM NAC for 15 min and then stimulated with 10 ng/ml TGF-β1 for 30 min. After 72h cells were lysed and subjected to immunoblot analysis for E-cadherin, N-Cadherin, α-SMA and β-actin. **D**. Photographs of cells treated as indicated were taken with a phase/contrast microscope. **E.** Representative images of cells treated as indicated, fixed and examined by immunofluorescence microscopy of phalloidin and E-cadherin. **F.** MCF-10A cells were pre-treated with 5 mM NAC or 5 μM DPI for 15 min before stimulation with 10ng/ml TGF-β1 for 90 min. Total RNA was extracted and SNAIL1 mRNA levels were analyzed by qRTPCR. Results are representative of three experiments. ∗p<0.005 treatment *vs* control. The primers used are shown in Table I.

Fig. 2. Nuclear ROS induced by TGF β1 require the histone demethylase, LSD1. A. Immunofluorescence detection of 8-oxoG by fluorescein-tagged 8-oxoG-binding protein of cells pre-treated with 5 mM NAC or 5μM DPI for 15 min before stimulation with 10 ng/ml TGF-β1 for 30 min. **B.** LSD1 targeting by siRNA reduces LSD1 mRNA in MCF10A cells. A specific siRNA targeting LSD1 or a scrambled siRNA was electroporated in MCF10A cells as described in Materials and Methods. 72 h later, total RNA was extracted, reverse transcribed, and amplified with specific primers to human LSD1 and a reference gene (β-actin or 18SRNA). The normalized data derive from at least 3 experiments. **C.** Immunofluorescence of 8-oxoG binding protein in control or 24 h LSD1-depleted cells, pre-treated with 5 mM NAC for 15 min before stimulation with 10ng/ml TGF-β1 for 90 min. **D.** Immunofluorescence microscopy of phalloidin and E-cadherin in control or LSD1-depleted cells exposed to 10ng/ml TGFβ1 for 90 min. The primers used are shown in Table I.

Fig. 3. LSD1 represses *SNAIL1* expression.

A. LSD1 was depleted in MCF-10A (shLSD1) for 72 h (Fig.S2) and stimulated with 10 ng/ml TGF-β1 for 90 min (inset). Total RNA was extracted and SNAIL1 or LSD1 (inset) mRNA expression levels were analyzed by qRT-PCR. Results are representative of three experiments: * p<0.005 TGF-β1 *vs* control; ** p<0.005 shRNA LSD1+TGF-β1 *vs* TGF-β1. **B.** Cells were transiently transfected with expression vectors encoding wild type human LSD1wild type (wtLSD1) or a dominant negative mutant at threonine 110 (mutALA) or the 54phospho-mimetic mutant at the same site (mutASP) (13, 23) for 48 h. After stimulation with 10 ng/ml TGF-β1 for 90 min, total RNA was extracted and SNAIL1 mRNA expression was analyzed by qRT-PCR.

Results are representative of three experiments: * p<0.005 transfected cells *vs* control. **C** and **D.** Basal and TGF-β1-induced SNAIL1 are altered in cells expressing LSD1 mutants. SNAIL1 mRNA analysis was carried out by qPCR with specific primers and normalized to 18S RNA. Panel D shows the normalized induction at 90 min TGFβ−1. * p<0.001 transfected cells *vs* control (mock).** p<0.005 cells expressing wtLSD1 *vs* mutALA. The primers used are shown in Table I.

Fig. 4. TGF-β1 at the *SNAIL1* promoter induces histone H3-k4 and k9 methylation changes, loss of LSD1 and recruitment of *JMJD2A*.

Chromatin from MCF-10A cells, stimulated with 10 ng/ml TGF-β1 for 30 min, was immune-precipitated with –anti-H3 (A) anti-H3k4me2/3 (B) or anti anti-H3kme2/3 (C) or anti-LSD1 or JMJD2A (D) antibodies. The region encompassing the SNAIL1 promoter (see Materials and Methods) and a region in a gene not induced by TGF-β1, human TSH receptor gene (Fig.S5) were amplified by RT-PCR. Normal mouse preimmune IgG was used as a negative control. The bar graph shows the qPCR signals in immunoprecipitates, normalized to input DNA and histone H3 content from each sample. Data are reported as mean±SD of three experiments. * p<0.005 TGF-β1 stimulated cells *vs* control; ** p<0.001 90 or 60 min TGF-β1 stimulated cells *vs* 30 min. The primers used are shown in Table I.

Fig. 5. TGF-β1 at the *WIF1* promoter induces histone H3-k4 and k9 methylation changes and recruitment of LSD1.

Chromatin from MCF-10A cells stimulated with 10 ng/ml TGF-β1 for 30 min was immune-precipitated with–anti-H3 (A) anti-H3k4me2/3 (B) or anti anti-H3k9me2/3 (C) or anti-LSD1 or JMJD2A (D) antibodies. The region encompassing the *WIF1* promoter (see Materials and

Methods) and a region in two genes not induced by TGFβ1 (Fig.S5) were amplified by RT-PCR. Normal mouse pre-immune IgG was used as a negative control. The bar graph shows the qPCR signals in immunoprecipitates, normalized to input DNA and histone H3 content from each sample. Data are reported as mean±SD of three experiments. * p<0.005 TGF-β1 stimulated cells *vs* control; ** p<0.001 60 or 90 min TGF-β1 stimulated cells *vs* 30 min TGF-β1. The primers used are shown in Table I.

Fig. 6. Loss or gain of repressors at *SNAIL1* and *WIF1* promoters, respectively.

Phosphorylated SMAD2/3 induced by TGF-β1 binds and recruits JMJD2A allowing LSD1 depletion from the *SNAIL1* promoter. Chromatin from MCF-10A cells stimulated with 10 ng/ml TGF-β1 for 30 min was precipitated with–anti-NcoR1 or HDAC3 (**A** and **B**) antibodies and amplified by qPCR with primers corresponding to the *SNAIL1* gene (**A**) or *WIF1* (**B**) promoters and the same region in two genes not induced by TGF-β1 (Fig.S5) were amplified by RT-PCR. **C** and **D** show ChIP analysis of SMAD2-3 and phosphorylated SMAD2-3 at the *SNAIL1* and *WIF1* promoters, respectively. Normal mouse pre-immune IgG was used as a negative control. The bar graph shows the qPCR signals in immunoprecipitates, normalized to input DNA and histone H3 content from each sample. Data are reported as mean±SD of three experiments. * p<0.005 TGF-β1 stimulated cells *vs* control; ** p<0.001 90 or 30 min TGF-β1 stimulated cells *vs* 60 min TGF-β1**. E** and **F** show the immunoprecipitation of total cell extracts with antiSMAD2-3 antibodies and immunoblot with anti JMJD2A I or LSD1 (**F**) antibodies. Briefly, MCF-10A cells were stimulated with 10 ng/ml TGF-β1 for the indicated times. Cells were lysed and Smad2/3 was immunoprecipitated and separated and immunoblotted with anti-JMJD2A or LSD1 antibodies. The bar graph derives from the densitometric scanning of the gel band normalized to the fraction of SMAD2-3 immunoprecipitated. The primers used are shown in Table I.

Fig. 7. Cyclical oscillations of H3 histone methylation, recruitment of BER and demethylases at promoters of TGF-β1 activated and repressed genes.

Summary of the ChIP and RNA expression data at various times after TGF-β1 exposure of MCF10A cells. On the left are shown ChIP and RNA data expressed in arbitrary units relative to SNAIL1 or WIF1 gene, respectively. On the right are shown the proteins analyzed (color-coded). Peaks of chromatin recruitment of LSD1 (red) and JMJD2A (green) are indicated in the second and third row from the top.

Supplementary Figures

Figure S1. TGF-β1 induces *SNAIL1* expression .

RNA analysis of *SNAIL1* gene following TGF-β1 exposure. MCF-10A cells were stimulated with 10 ng/ml TGF-β1 for the indicated times, total RNA isolated, reverse transcribed and amplified by qPCR with specific primers. The values were normalized to 18S RNA. The experiments were repeated three times in triplicate. *p<0.01 as compared to control (0). **p<0.01 as compared to 30 min TGF-β1. The primers used are shown in Table I.

Figure S2. LSD1 silencing.

MCF10A cells were transfected with an expression vector encoding shRNA targeting LSD1 and 72 h later were treated with 10 ng/ml TGF-β1 for the indicated times. Total RNA was extracted, reverse transcribed and amplified by qPCR with LSD1 specific primers. The values were normalized to 18S RNA .* p<0.01 as compared to control (0) transfected with scrambled shRNA; ** p<0.01 as compared to 90 min TGF-β1 transfected with scrambled shRNA. The primers used are shown in Table I.

Figure S3. TGF- β 1 inhibits WIF1 expression through LSD1

MCF10A cells were transfected with an expression vector encoding shRNA targeting LSD1 and 72 h later were treated with 10 ng/ml TGF-β1 for the indicated times. Total RNA was extracted, reverse transcribed and amplified by qPCR with WIF1 and LSD1 specific primers. The values were normalized to 18SRNA .* p<0.01 as compared to control (0) transfected with scrambled shRNA; ** p<0.01 as compared to 90 min TGFβ1 transfected with scrambled shRNA. The primers used are shown in Table I.

Figure S4. Tranylcypromine or Parnate, a LSD1 catalytic inhibitor, blunts TGFβ1 *SNAIL1* induction and relieves *WIF1* silencing.

MCF10A cells were pre-treated with tranylcypromine or parnate (1 ug/ml) for 60 min and stimulated with 10 ng/ml TGF-β1 for the indicated times. Total RNA isolated, reverse transcribed and amplified by qPCR with specific primers. The values were normalized to 18SRNA or GADPH. A and B show *SNAIL1* and *WIF1* mRNA quantification, respectively. *p<0.01 as compared to untreated control (0). **p<0.01 as compared to treated-samples before TGF-β1 treatment. The primers used are shown in Table I.

Fig.S5. TGF-β1does not modify H3 methylation or LSD1-JMJD2A recruitment at a control gene, *TSHR* .

MCF10A cells were stimulated with 10 ng/ml TGF-β1 for the indicated times. ChIP analysis with anti H3, H3k4me2-me3, H3k9me2-me3, LSD1 and JMJD2A antibodies as indicated in each panel. The primer used for the reference gene, TSH receptor, is shown in Table I.

Figure S6. TGF-β1 induces recruitment of OGG1 and APE1 at both induced and repressed promoters

MCF10A cells were stimulated with 10 ng/ml TGF-β1 for the indicated times. ChIP analysis with anti OGG1 and APE1 antibodies was performed as described in Materials and Methods. The regions analyzed are the promoters of *SNAIL1* (A), *WIF1* (B) and *TSHR* (C), as indicated in Table I. * p<0.001 TGF-β1 stimulated cells *vs* control; ** p<0.001 TGF-β1 stimulated cells 60 min *vs* 30 min. The primers used are shown in Table I.

Fig.S7. JMJD2A silencing impairs TGFβ-1 induced EMT but not TGF-β1 production of ROS.

MCF10A cells were transfected with specific siRNA targeting JMJD2A and were stimulated with TGF-β-1 72 h later in the presence or absence of NAC as indicated in Fig.1 and 2. In **A** is shown the immunofluorescence of oxoG binding protein as illustrated in Fig.2. **B** shows the quantitative analysis of the same samples shown in A an indicated below the histogram, **C** shows the immunofluorescence of a representative image of control or JMJD2A-silenced cells induced with 10 ng/ml TGF-β1 for 30 min, fixed and examined by immunofluorescence for Phalloidin and E-cadherin staining. **D** shows the image quantification of SNAIL1 expression as illustrated in Materials and Methods. **E** shows JMJD2A RNA analysis in cells transfected with siRNA targeting JMJD2A. * p<0.001 TGF-β1 stimulated cells *vs* control; # p<0.001 control scrambled *vs* siRNA JMJD2A in TGF-β1 stimulated cells. The primers used are shown in Table I.

Figure S8. TGFβ-1 induces the recruitment at *SNAIL1* and *WIF1* promoter sites of the histone methyl transferases, SUV39- SET9.

ChIP analysis of cells exposed to TGF-β1 for the indicated times and processed for

ChIP analysis with antibodies specific to SUV39 and SET9. The regions analyzed are SNAIL 1, WIF1 and TSHR promoters. The primers used are shown in Table I.

Figure S9. Re-ChIP analysis of SMAD2-3 immunoprecipitates at the *SNAIL1* and *WIF1* promoters. A. ChiP performed with anti-SMAD2-3 immunoprecipitates at SNAIL1 or WIF promoters were re-ChIPPed with anti JMJD2A (B) or anti-LSD1 (C) antibodies. Cells were stimulated with TGF-β1 for the indicated times and processed as described in Materials and Methods. Re-Chipped values are plotted as % of the first ChIP shown in A. The primers used are shown in Table I.

Figure S10. TGFβ-1 controls the levels of LSD1 protein. Cells were stimulated with TGF-β-1(10 ng/ml) and the extracts collected and analyzed by immunoblot with specific antibodies to LSD1 (**A**) and JMJD2A (**B**). The upper panels show the quantitative analysis of at least 3 experiments. **C** and **D** show the same experiment in which the cells were pre-treated with the proteasome inhibitor, MG132 (10 ug/ml) for the period indicated in the presence or absence of TGFβ-1.

7. REFERENCES

[1] Gary Greenburg and Elizabeth D. Hay "Epithelia Suspended in Collagen Gels Can Lose Characteristics of Migrating Mesenchymal Cells Polarity and Express" J Cell Biol. 1982 Oct;95(1):333-9

[2] Rivka C. Stone, Irena Pastar, Nkemcho Ojeh1, Vivien Chen, Sophia Liu, Karen I. Garzon, Marjana Tomic-Canic "Epithelial-mesenchymal transition in tissue repethilatioair and fibrosis" Cell Tissue Res DOI 10.1007/s00441-016-2
464-0

[3] Kalluri R[1], Neilson EG. "Epithelial-mesenchymal transition and its implications for fibrosis." J Clin Invest. 2003 Dec;112(12):1776-84.

[4] Ruby Yun-Ju Huang, Parry Guilford, Jean Paul Thiery "Early events in cell adhesion and polarity during epithelial-mesenchymal transition" J Cell Sci 2012 125: 4417-4422; doi: 10.1242/jcs.099697

[5] Thiery JP, Sleeman JP "Complex networks orchestrate epithelial-mesenchymal transitions." Nat Rev Mol Cell Biol 2006 7:131–142

[6] Maschler S, Wirl G, Spring H, Bredow DV, Sordat I, Beug H, Reichmann E "Tumor cell invasiveness correlates with changes in integrin expression and localization". Oncogene 2005 24:2032–2041

[7] Jordan NV, Johnson GL, Abell AN "Tracking the intermediate stages of epithelial-mesenchymal transition in epithelial stem cells and cancer." Cell Cycle 2011 10:2865–2873

[8] Rivka C. Stone, Irena Pastar, Nkemcho Ojeh1, Vivien Chen, Sophia Liu, Karen I. Garzon, Marjana Tomic-Canic "Epithelial-mesenchymal transition in tissue repair and fibrosis" Cell Tissue Res DOI 10.1007/s00441-016-2464-0

[9] Baum CL, Arpey CJ "Normal cutaneous wound healing: clinical correlation with cellular and molecular events". 2005 Dermatol Surg 31:674–686. discussion 686

[10] Santoro MM, Gaudino G "Cellular and molecular facets of keratinocyte reepithelization during wound healing". 2005 Exp Cell Res 304:274–286

[11] Hudson LG, Newkirk KM, Chandler HL, Choi C, Fossey SL, Parent AE, Kusewitt DF "Cutaneous wound reepithelialization is compromised in mice lacking functional Slug (Snai2)". 2009 J Dermatol Sci 56:19–26

[12] Savagner P, Kusewitt DF, Carver EA, Magnino F, Choi C, Gridley T, Hudson LG "Developmental transcription factor slug is required for effective re-epithelialization by adult keratinocytes". 2005 J Cell Physiol 202:858–866

[13] Savagner P "Leaving the neighborhood: molecular mechanisms involved during epithelial-mesenchymal transition. Bioessays" 2001 23:912–923

[14] Savagner P, Kusewitt DF, Carver EA, Magnino F, Choi C, Gridley T, Hudson LG "Developmental transcription factor slug is required for effective re-epithelialization by adult keratinocytes." 2005 J Cell Physiol 202:858–866

[15] Krainock M, Toubat O, Danopoulos S, Beckham A, Warburton D, Kim R "Epicardial epithelial-to-mesenchymal transition in heart development and disease." 2016 J Clin Med 5:27

[16] Krainock M, Toubat O, Danopoulos S, Beckham A, Warburton D, Kim R "Epicardial epithelial-to-mesenchymal transition in heart development and disease." 2016 J Clin Med 5:27

[17] Rivka C. Stone, Irena Pastar, Nkemcho Ojeh1, Vivien Chen, Sophia Liu, Karen I. Garzon, Marjana Tomic-Canic "Epithelial-mesenchymal transition in tissue repair and fibrosis" Cell Tissue Res DOI 10.1007/s00441-016-2464-0

[18] Iwano M, Plieth D, Danoff TM, Xue C, Okada H, Neilson EG "Evidence that fibroblasts derive from epithelium during tissue fibrosis." 2002 J Clin Invest 110:341–350

[19] Rastaldi MP, Ferrario F, Giardino L, Dell'Antonio G, Grillo C, Grillo P, Strutz F, Muller GA, Colasanti G, D'Amico G "Epithelial-mesenchymal transition of tubular epithelial cells in human renal biopsies." 2002 Kidney Int 62:137–146

[20] Fan JM, Ng YY, Hill PA, Nikolic-Paterson DJ, Mu W, Atkins RC, Lan HY "Transforming growth factor-beta regulates tubular epithelial-myofibroblast transdifferentiation in vitro" 1999 Kidney Int 56:1455–1467

[21] Chapman HA "Epithelial-mesenchymal interactions in pulmonary fibrosis". 2011 Annu Rev Physiol 73:413–435

[22] Kim KK, Kugler MC, Wolters PJ, Robillard L, Galvez MG, Brumwell AN, Sheppard D, Chapman HA "Alveolar epithelial cell mesenchymal transition develops in vivo during pulmonary fibrosis and is regulated by the extracellular matrix." 2006 Proc Natl Acad Sci U S A 103:13180–13185

[23] Willis BC, Liebler JM, Luby-Phelps K, Nicholson AG, Crandall ED, du Bois RM, Borok Z "Induction of epithelial-mesenchymal transition in alveolar epithelial cells by transforming growth factor-beta1: potential role in idiopathic pulmonary fibrosis." 2005 Am J Pathol 166:1321–1332

[24] Limana F, Zacheo A, Mocini D, Mangoni A, Borsellino G, Diamantini A, De Mori R, Battistini L, Vigna E, Santini M, Loiaconi V, Pompilio G, Germani A, Capogrossi MC "Identification of myocardial and vascular precursor cells in human and mouse epicardium". 2007 Circ Res 101:1255–1265

[25] Smart N, Dube KN, Riley PR "Epicardial progenitor cells in cardiac regeneration and neovascularisation." Vasc Pharmacol 2013 58:164–173

[26] Kaimori A, Potter J, Kaimori JY, Wang C, Mezey E, Koteish A "Transforming growth factor-beta1 induces an epithelial-to-mesenchymal transition state in mouse hepatocytes in vitro". 2007 J Biol Chem 282:22089–22101

[27] Thiery, J. P. Epithelial–mesenchymal transitions in tumour progression. (2002) *Nature Rev. Cancer* 2, 442–454.

[28] Ansieau, S. *et al*. Induction of EMT by twist proteins as a collateral effect of tumor-promoting inactivation of premature senescence. (2008) *Cancer Cell* 14, 79–89

[29] Mejlvang, J. *et al*. Direct repression of cyclin D1 by SIP1 attenuates cell cycle progression in cells undergoing an epithelial mesenchymal transition. (2007) *Mol. Biol. Cell*18, 4615–4624

[30] Thiery, J. P., Acloque, H., Huang, R. Y. & Nieto, M. A. Epithelial–mesenchymal transitions in development and disease. *Cell* 139, 871–890(2009).

[31]Marcucci F, Stassi G, De Maria R. "Epithelial-mesenchymal transition: a new target in anticancer drug discovery" (2016) Nat Rev Drug Discov. 2016 May;15(5):311-25.

[32] Dumont, N. *et al*. "Sustained induction of epithelial to mesenchymal transition activates DNA methylation of genes silenced in basal-like breast cancers". (2008) *Proc. Natl Acad. Sci. USA* 105, 14867–14872

[33] Marcucci F, Stassi G, De Maria R. "Epithelial-mesenchymal transition: a new target in anticancer drug discovery" (2016) Nat Rev Drug Discov. 2016 May;15(5):311-25.

[34] Marcucci, F., Bellone, M., Caserta, C. A. & Corti, A. Pushing tumor cells towards a malignant phenotype: stimuli from the microenvironment, intercellular communications and alternative roads. (2014) *Int. J. Cancer* 135,1265–1276

[35] Todaro, M. *et al*. "CD44v6 is a marker of constitutive and reprogrammed cancer stem cells driving colon cancer metastasis". 2014 *Cell Stem Cell* 14, 342–356.

[36] Lemmon MA, Schlessinger J "Cell signaling by receptor tyrosine kinases". 2010 Cell 141:1117–1134

[37] Tsai JH, Yang J "Epithelial-mesenchymal plasticity in carcinoma metastasis". 2013 Genes Dev 27:2192–2206

[38] Derynck R, Zhang YE "Smad-dependent and Smad-independent pathways in TGF-beta family signalling." 2003 Nature 425:577–584

[39] Derynck R, Zhang YE "Smad-dependent and Smad-independent pathways in TGF-beta family signaling". 2003 Nature 425:577–584

[40] Derynck, R. & Feng, X.-H. TGFβ receptor signaling. *Biochim. Biophys. Acta*1333, F105−F150 (1997)

[41] Derynck R, Zhang YE "Smad-dependent and Smad-independent pathways in TGF-beta family signaling". 2003 Nature 425:577–584

[42] Massagué, J. "How cells read TGF-β signals." 2000 *Nature Rev. Mol. Cell Biol.* 1, 169−178

[43] Itoh, S., Itoh, F., Goumans, M. J. & ten Dijke, P. "Signaling of transforming growth factor-β family members through Smad proteins". 2000 *Eur. J. Biochem.*267, 6954−6967

[44] Derynck R, Zhang YE “Smad-dependent and Smad-independent pathways in TGF-beta family signaling”. 2003 Nature 425:577–584

[45] Moustakas, A., Souchelnytskyi, S. & Heldin, C.-H. Smad regulation in TGF-β signal transduction. 2001 *J. Cell Sci.* 114, 4359−4369

[46] Itoh, S., Itoh, F., Goumans, M. J. & ten Dijke, P. “Signaling of transforming growth factor-β family members through Smad proteins”. 2000 *Eur. J. Biochem.*267, 6954−6967

[47] Derynck R, Zhang YE “Smad-dependent and Smad-independent pathways in TGF-beta family signalling.” 2003 Nature 425:577–584

[48] Chen, C.-R., Kang, Y., Siegel, P. M. & Massagué, J. E2F4/5 and p107 as Smad cofactors linking the TGFβ receptor to c-myc repression. 2002 *Cell* 110, 19−32

[49] Griswold-Prenner, I., Kamibayashi, C., Maruoka, E. M., Mumby, M. C. & Derynck, R. “Physical and functional interactions between type I transforming growth factor β receptors and Bα, a WD-40 repeat subunit of phosphatase 2A.” 1998 *Mol. Cell. Biol.* 18, 6595−6604

[50] Derynck R, Zhang YE “Smad-dependent and Smad-independent pathways in TGF-beta family signaling”. 2003 Nature 425:577–584

[51] de Caestecker, M. P. *et al.* “Smad2 transduces common signals from receptor serine-threonine and tyrosine kinases”. 1998 *Genes Dev.* 12, 1587−1592

[52] Kretzschmar, M., Doody, J., Timokhina, I. & Massagué, J. “A mechanism of repression of TGF-/Smad signaling by oncogenic Ras.” 1999 *Genes Dev.* 13, 804−816

[53] Yu, L., Hebert, M. C. & Zhang, Y. E. “TGF-β receptor-activated p38 MAP kinase mediates Smad-independent TGF- responses”. 2002 *EMBO J.*21, 3749−3759

[54] Zavadil, J. *et al.* “Genetic programs of epithelial cell plasticity directed by transforming growth factor-β”. 2001 *Proc. Natl Acad. Sci. USA*98, 6686−6691

[55] Tam WL, Weinberg RA. “The epigenetics of epithelial-mesenchymal plasticity in cancer.” 2013 *Nature medicine* 19(11):1438-1449. doi:10.1038/nm.3336.

[56] Agger, K., Christensen, J., Cloos, P.A. & Helin, K. “The emerging functions of histone demethylases.” 2008 *Curr. Opin. Genet. Dev.* **18**, 159–168

[57] Peinado, H., Olmeda, D. & Cano, A. “Snail, Zeb and bHLH factors in tumour progression: an alliance against the epithelial phenotype?” 2007 *Nat. Rev. Cancer* **7**, 415–428

[58] Shi, Y. *et al*. “Histone demethylation mediated by the nuclear amine oxidase homolog LSD1.” 2004 *Cell* **119**, 941–953

[59] Lim, S. *et al*. “Lysine-specific demethylase 1 (LSD1) is highly expressed in ER-negative breast cancers and a biomarker predicting aggressive biology”. 2010 *Carcinogenesis* **31**, 512–520.

[60] Harris, W.J. *et al*. “The histone demethylase KDM1A sustains the oncogenic potential of MLL-AF9 leukemia stem cells”. 2012 *Cancer Cell* **21**, 473–487

[61] Wang, Y. *et al*. “LSD1 is a subunit of the NuRD complex and targets the metastasis programs in breast cancer.” 2009 *Cell* **138**, 660–672.

[62] Metzger, E. *et al*. “LSD1 demethylates repressive histone marks to promote androgen-receptor–dependent transcription.” 2005 *Nature* **437**, 436–439

[63] Cedar, H. & Bergman, Y. Linking “DNA methylation and histone modification: patterns and paradigms.” 2009 *Nat. Rev. Genet.* **10**, 295–304

[64] Savagner, P., Yamada, K.M. & Thiery, J.P. The zinc-finger protein slug causes desmosome dissociation, an initial and necessary step for growth factor-induced epithelial-mesenchymal transition. 1997 *J. Cell Biol.* **137**, 1403–1419

[65] Vallés, A.M. *et al*. “Acidic fibroblast growth factor is a modulator of epithelial plasticity in a rat bladder carcinoma cell line”. 1990 *Proc. Natl. Acad. Sci. USA* **87**, 1124–1128

[66] Tam WL, Weinberg RA. “The epigenetics of epithelial-mesenchymal plasticity in cancer.” 2013 *Nature medicine* 19(11):1438-1449. doi:10.1038/nm.3336

[67] Paznekas WA, Okajima K, Schertzer M, Wood S, Jabs EW "Genomic organization, expression, and chromosome location of the human SNAIL gene (SNAI1) and a related processed pseudogene (SNAI1P)". 1999 *Genomics*. 62 (1): 42–9.

[68] Grau, Y., Carteret, C. & Simpson, P. Mutations and chromosomal rearrangements affecting the expression of *snail*, a gene involved in embryonic patterning in *Drosophila melanogaster*. *Genetics* 108, 347–360 (1984).

[69] Hammerschmidt, M. & Nüsslein-Volhard, C. "The expression of a zebrafish gene homologous to *Drosophila snail* suggests a conserved function in invertebrate and vertebrate gastrulation." 1993 *Development* 119, 1107–1118

[70] Cano, A. *et al*. "The transcription factor snail controls epithelial–mesenchymal transitions by repressing *E-cadherin* expression." 2000 *Nature Cell Biol.* 2, 76–83

[71] Batlle, E. *et al*. The transcription factor snail is a repressor of *E-cadherin* gene expression in epithelial tumour cells. 2000 *Nature Cell Biol.* 2, 84–89

[72] Carver, E. A., Jiang, R., Lan, Y., Oram, K. F. & Gridley, T. "The mouse *Snail* gene encodes a key regulator of the epithelial–mesenchymal transition." 2001 *Mol. Cell. Biol.* 21, 8184–8188

[73] Cano, A. *et al*. "The transcription factor snail controls epithelial–mesenchymal transitions by repressing *E-cadherin* expression." 2000 *Nature Cell Biol.* 2, 76–83

[74] Cano, A. *et al*. "The transcription factor snail controls epithelial–mesenchymal transitions by repressing *E-cadherin* expression." 2000 *Nature Cell Biol.* 2, 76–83.

[75] Hsieh J.C. "A new secreted protein that binds to Wnt proteins and inhibits their activities." 1999 Nature 398:431-436.

[76] Jen-Chih Hsieh, Laurent Kodjabachian, Martha L.Rebbert, Amir Rattner, Philip M. Smallwood, Cynthia Harryman Samos, Roel Nussel, Igor B.Dawid & Jeremy Nathans "A new secreted protein that binds to Wnt proteins and inhibits their activities" 1999 Nature Vol. 398

[77] Ling L. "Wnt signaling controls the fate of mesenchymal stem cells." 2009 Gene 433:1-7

[78] T Zhan, N Rindtorff, M Boutros "Wnt signaling in cancer" 2016 Oncogene doi: 10.1038/onc.2016.304

[79] Andrew S. Brack, Michael J. Conboy, Sudeep Roy, Mark Lee, Calvin J. Kuo, Charles Keller, Thomas A. Rando Increased Wnt Signaling During Aging Aletrs Muscle Stem Cell Fate and Increases Fibrosis

[80] Svegliati S, Marrone G, Pezone A, Spadoni T, Grieco A, Moroncini G, Grieco D, Vinciguerra M, Agnese S, Jüngel A, Distler O, Musti AM, Gabrielli A, Avvedimento EV "Oxidative DNA damage induces the ATM-mediated transcriptional suppression of the Wnt inhibitor WIF-1 in systemic sclerosis and fibrosis." 2014 Sci Signal. Sep 2;7(341):ra84.

[81] Stephen L Chan', Yan Cui' , Andrew van Hasselt, Hongyu Li, Gopesh Srivastava, Hongchuan Jin, Ka M Ng, Yajun Wang, Kwan Y Lee, George S W Tsao, Sheng Zhong, Keith D Robertson, Sun Y Rha, Anthony T C Chan and Qian Tao "The tumor suppressor Wnt inhibitory factor 1 is frequently methylated in nasopharyngeal and esophageal carcinomas" 2007 *Laboratory Investigation* 87, 644–650

[82] Mazieres J. "Wnt inhibitor Factor-1 is silenced by promoter hypermethylation in human lung cancers." Canc Res 2004; 64:4717-4720

[83] Wissmann C. WIF1, a component of the Wnt pathway, is downregulated in prostate, breast, lung and bladder cancer. J Pathol 2003;201:204-212

[84] Svegliati S, Marrone G, Pezone A, Spadoni T, Grieco A, Moroncini G, Grieco D, Vinciguerra M, Agnese S, Jüngel A, Distler O, Musti AM, Gabrielli A, Avvedimento EV "Oxidative DNA damage induces the ATM-mediated transcriptional suppression of the Wnt inhibitor WIF-1 in systemic sclerosis and fibrosis." 2014 Sci Signal. Sep 2;7(341):ra84.

[85]Zhang J[1], Tian XJ[2], Xing J[3]. "Signal Transduction Pathways of EMT Induced by TGF-β, SHH, and WNT and Their Crosstalks." 2016 J Clin Med. Mar 28;5(4).

[86] Cannito S, Novo E, Compagnone A, Valfre di BL, Busletta C, Zamara E, Paternostro C, Povero D, Bandino A, Bozzo F, Cravanzola C, Bravoco V, Colombatto S, Parola M 2008 "Redox mechanisms switch on hypoxia dependent epithelial-mesenchymal transition in cancer cells." Carcinogenesis 29: 2267-2278. 10.1093/carcin/bgn216.

[87] Rhyu DY, Yang Y, Ha H, Lee GT, Song JS, Uh ST, Lee HB (2005) Role of reactive oxygen species in TGF-beta1-induced mitogen-activated protein kinase activation and epithelial-mesenchymal transition in renal tubular epithelial cells. J Am Soc Nephrol 16: 667-675.

[88] Parri M, Chiarugi P "Redox molecular machines involved in tumor progression." 2013 Antioxid Redox Signal 19: 1828-1845.

[89] Cirri P, Chiarugi P "Cancer-associated-fibroblasts and tumour cells: a diabolic liaison driving cancer progression." 2012 Cancer Metastasis Rev 31: 195-208.

[90] Giannoni E, Bianchini F, Masieri L, Serni S, Torre E, Calorini L, Chiarugi P (2010) Reciprocal activation of prostate cancer cells and cancer-associated fibroblasts stimulates epithelial-mesenchymal transition and cancer stemness. Cancer Res 70: 6945-6956.

[91] Perillo B, Ombra MN, Bertoni A, Cuozzo C, Sacchetti S, Sasso A, Chiariotti L,Malorni A, Abbondanza C, Avvedimento EV "DNA oxidation as triggered by H3K9me2 demethylation drives estrogen-induced gene expression." 2008 Science 319: 202-206.

[92] Zuchegna C, Aceto F, Bertoni A, Romano A, Perillo B, Laccetti P, Gottesman ME, Avvedimento EV, Porcellini A. "Mechanism of retinoic acidinduced transcription: histone code, DNA oxidation and formation of chromatin loops." 2015 Nucleic Acids Res. 42:11040-55.

[93] Svegliati S, Marrone G, Pezone A, Spadoni T, Grieco A, Moroncini G, Grieco D, Vinciguerra M, Agnese S, Jüngel A, Distler O, Musti AM, Gabrielli A, Avvedimento EV. "Oxidative DNA damage induces the ATM-mediated transcriptional suppression of the Wnt inhibitor WIF1 in systemic sclerosis and fibrosis." 2014 Sci Signal: 7(341):ra84.

[94] Fan Jiang, Guei-Sheung Liu, Gregory J. Dusting, YElsa C. Chan "NADPH oxidase dependent redox signaling in TGF-β-mediated fibrotic responses." 2014 Redox Biology : 2, 67–272.

[95] Amente, S, Lania, L and Majello, B. (2013) The histone LSD1 demethylase in stemness and cancer transcription programs. Biochimica et Biophysica Acta (BBA) - Gene Regulatory Mechanisms, 1829, 981-986.

[96] Lin T1, Ponn A, Hu X, Law BK, Lu J. (2010) Requirement of the histone demethylase LSD1 in Snai1-mediated transcriptional repression during epithelial-mesenchymal transition. Oncogene.;29:4896-904.

[97] Lin T1, Ponn A, Hu X, Law BK, Lu J. (2010) Requirement of the histone demethylase LSD1 in Snai1-mediated transcriptional repression during epithelial-mesenchymal transition. Oncogene.;29:4896-904.

[98] Zuchegna C, Aceto F, Bertoni A, Romano A, Perillo B, Laccetti P, Gottesman ME, Avvedimento EV, Porcellini A. (2015) Mechanism of retinoic acid induced transcription: histone code, DNA oxidation and formation of chromatin loops. Nucleic Acids Res. 42:11040-55.

[99] Amente S, Bertoni A, Morano A, Lania L, Avvedimento EV, Majello B (2010) LSD1-mediated demethylation of histone H3 lysine 4 triggers Myc-induced transcription. Oncogene 29: 3691-3702.

[100] Ambrosio R, Damiano V, Sibilio A, De Stefano MA, Avvedimento VE, Salvatore D, Dentice M.(2013) Epigenetic control of type 2 and 3 deiodinases in myogenesis: role of Lysine-specific Demethylase enzyme and FoxO3. Nucleic Acids Res. 2013 Apr 1;41(6):3551-62.

[101] Yu-Jiang Shi, YCaitlin Matson, YFei, Lan, Shigeki Iwase, Tadashi Baba, YYang Shi.(2005). Regulation of LSD1 Histone Demethylase Activity by Its Associated Factors. Molecular Cell:19, 857–864

[102] J.-F. Couture., E. Collazo., P. A Ortiz-Tello1, J. S Brunzelle2 and R.C Trieve (2007) Specificity and mechanism of JMJD2A, a trimethyllysine-specific histone demethylase Nat. Struct.&Mol.Biol. 14, 689 - 695

[103] Lin T1, Ponn A, Hu X, Law BK, Lu J. (2010) Requirement of the histone demethylase LSD1 in Snai1 mediated transcriptional repression during epithelial-mesenchymal transition. Oncogene.;29:4896-904.

[104] Sidorenko VS1, Nevinsky GA, Zharkov DO. (2007) Mechanism of interaction between human 8oxoguanine-DNA glycosylase and AP endonuclease. DNA Repair (Amst) 6(3):317-28. PMID: 17126083.

[105] Nishioka K1, Chuikov S, Sarma K, Erdjument-Bromage H, Allis CD, Tempst P, Reinberg D.(2002) Set9, a novel histone H3 methyltransferase that facilitates transcription by precluding histone tail modifications required for heterochromatin formation. Genes Dev: 16:479-89.

[106] Fritsch, L, Robin,P, Mathieu, J. R.R., Souidi M., Hinaux, H., Rougeulle, C, Harel-Bellan, A, Ameyar-Zazoua, M, Ait-Si-Ali,S. "A Subset of the Histone H3 Lysine 9 Methyltransferases Suv39h1, G9a, GLP, and SETDB1 Participate in a Multimeric Complex Mol."2010 Cell., 37, 46-56.

[107] Yiwei Lin, Chenfang Dong, and Binhua P. Zhou (2014) Epigenetic Regulation of EMT: The Snail Story. Curr Pharm Des. : 20: 1698–1705.

[108] Perillo B, Ombra MN, Bertoni A, Cuozzo C, Sacchetti S, Sasso A, Chiariotti L, Malorni A, Abbondanza C, Avvedimento EV (2008) DNA oxidation as triggered by H3K9me2 demethylation drives estrogen-induced gene expression. Science 319: 202-206.

[109] Amente S, Bertoni A, Morano A, Lania L, Avvedimento EV, Majello B (2010) LSD1-mediated demethylation of histone H3 lysine 4 triggers Myc-induced transcription. Oncogene 29: 3691-3702.

[110] Wrighton, KH, Lin, X and Feng X (2009) Phospho-control of TGF-β superfamily signaling. Cell Res.

[111] Javaid S, Zhang J, Anderssen E, Black JC, Wittner BS, Tajima K, Ting DT, Smolen GA, Zubrowski M, Desai R, Maheswaran S, Ramaswamy S, Whetstine JR, Haber DA.(2013). Dynamic chromatin modification sustains epithelialmesenchymal transition following inducible expression of Snail-1. Cell Rep.: 26:1679-89.

[112] Perillo B, Ombra MN, Bertoni A, Cuozzo C, Sacchetti S, Sasso A, Chiariotti L, Malorni A, Abbondanza C, Avvedimento EV (2008) DNA oxidation as triggered by H3K9me2 demethylation drives estrogen-induced gene expression. Science 319: 202-206.

[113] Zuchegna C, Aceto F, Bertoni A, Romano A, Perillo B, Laccetti P, Gottesman ME, Avvedimento EV, Porcellini A. (2015) Mechanism of retinoic acid induced transcription: histone code, DNA oxidation and formation of chromatin loops. Nucleic Acids Res. 42:11040-55.

[114] Amente S, Bertoni A, Morano A, Lania L, Avvedimento EV, Majello B (2010) LSD1-mediated demethylation of histone H3 lysine 4 triggers Myc-induced transcription. Oncogene 29: 3691-3702.

[115] Chiarugi P (2009) Survival or death: the redox paradox. Antioxid Redox Signal 11: 2651-2654.

[116] Cannito S, Novo E, di Bonzo LV, Busletta C, Colombatto S, Parola M (2010) Epithelial-mesenchymal transition: from molecular mechanisms, redox regulation to implications in human health and disease. Antioxid Redox Signal 12: 1383-1430.

[117] Fan Jiang[a], · Guei-Sheung Liu[b, c], Gregory J. Dusting[b, c], · YElsa C. Chan[b](2014) NADPH oxidase-dependent redox signaling in TGF-β-mediated fibrotic responses. Redox Biology : 2, 67–272.

[118] Wrighton, KH, Lin, X and Feng X (2009) Phospho-control of TGF-β superfamily signaling. Cell Res. :19,8-20

[119] Ramadoss S, Chen X, Wang CY. (2012) Histone demethylase KDM6B promotes epithelial-mesenchymal transition. J Biol Chem. : 287:44508-17

[120] Perillo B, Ombra MN, Bertoni A, Cuozzo C, Sacchetti S, Sasso A, Chiariotti L, Malorni A, Abbondanza C, Avvedimento EV (2008) DNA oxidation as triggered by H3K9me2 demethylation drives estrogen-induced gene expression. Science 319: 202-206.

[121] Zuchegna C, Aceto F, Bertoni A, Romano A, Perillo B, Laccetti P, Gottesman ME, Avvedimento EV, Porcellini A. (2015) Mechanism of retinoic acidinduced transcription: histone code, DNA oxidation and formation of chromatin loops. Nucleic Acids Res. 42:11040-55

[122] Fong YW1, Cattoglio C, Tjian R,. (2013) The intertwined roles of transcription and repair proteins. Mol Cell. : 52:291-302.

[123] Svegliati S, Marrone G, Pezone A, Spadoni T, Grieco A, Moroncini G, Grieco D, Vinciguerra M, Agnese S, Jüngel A, Distler O, Musti AM, Gabrielli A, Avvedimento EV.(2014) Oxidative DNA damage induces the ATM-mediated transcriptional suppression of the Wnt inhibitor WIF1 in systemic sclerosis and fibrosis. Sci Signal: 7(341):ra84.

Ringrazio il Prof. Gabrielli e il Prof. Avvedimento per avermi permesso di compiere questo viaggio nel meraviglioso mondo della ricerca. Ringrazio il Prof. Avvedimento per avermi permesso di lavorare ed apprendere nel suo laboratorio a Napoli.
Un pensiero a tutti i miei compagni di lavoro che sono diventati amici: Rita, Alfonso, Mariarosaria, Francesco, Francesca, Giuliana, Federica, Antonio, Laura, Rossella, Maria Sepe, Monia, Stefano, Maria Soprano, Giusi, Roberto, Roberta, James, Sara, Lucrezia, Simona, Ermanno, Olga, Francesco Pacifico, Domenico, Alessio, Eliana, Imma, Candina, la Dott.ssa Gallo, la Prof. Acquaviva, Mariarita, Michaela, Luigi e un grazie anche a te Carlos che ancora devi caricare quel gel (Alfonso ti vuole bene).
Con l'augurio che ognuno di voi possa sempre proseguire la sua Ricerca….
Un immancabile pensiero alla Società dei Piastrellatori e Piastrellatore Capo, con un grande abbraccio ad un Amico, a sua moglie e suo figlio che proprio ora stanno affrontando la loro battaglia più dura.
Mamma, Papà, Pippo vi voglio bene e mi avete sempre sostenuto anche a 400 km di distanza.
A Te.
A Napoli città misteriosa che mi ha regalato momenti di pura magia.